Accelerator Magnet Quench Heater Technology and Quality Control Tests for the LHC High Luminosity Upgrade

Bachelor Thesis

Presented by

Florian Meuter

Supervisor:

M. Sc. Christian Scheuerlein, CERN

Prof. Dr. Ing. Thomas Seifert,
University of Applied Sciences Offenburg

Eidesstattliche Versicherung

Hiermit versichere ich eidesstattlich, dass die vorliegende Bachelorthesis von mir selbstständig und ohne unerlaubte fremde Hilfe angefertigt worden ist, insbesondere, dass ich alle Stellen, die wörtlich oder annähernd wörtlich oder dem Gedanken nach aus Veröffentlichungen, unveröffentlichten Unterlagen und Gesprächen entnommen worden sind, als solche an den entsprechenden Stellen innerhalb der Arbeit durch Zitate kenntlich gemacht habe, wobei in den Zitaten jeweils der Umfang der entnommenen Originalzitate kenntlich gemacht wurde. Ich bin mir bewusst, dass eine falsche Versicherung rechtliche Folgen haben wird.

Offenburg, den 28. Februar 2017

Abstract

The High Luminosity upgrade of the Large Hadron Collider (HL-LHC) foresees the installation of new superconducting Nb_3Sn magnets. For the protection of these magnets, quench heaters are placed on the magnet coils. The quench heater circuits are chemically etched from a stainless steel foil that is glued onto a flexible Polyimide film, using flexible printed circuit production technology. Approximately 500 quench heaters with a total length of about 3000 m are needed for the HL-LHC magnets.

In order to keep the heater circuit electrical resistance in acceptable limits, an approximately 10 µm-thick Cu coating is applied onto the steel foil. The quality of this Cu coating has been found critical in the quench heater production. The work described in this thesis focuses on the characterisation of Cu coatings produced by electrolytic deposition, sputtering and electron beam evaporation.

The quality of the Cu coatings from different manufacturers has been assessed for instance by ambient temperature electrical resistance measurements, Residual Resistivity Ratio (RRR) measurements, adhesion tests. The tested electrolytic Cu coatings with Ni interlayer adhere well on the steel substrate, and they have the required room temperature and 4.2 K electrical resistivity. Electron beam evaporated Cu coatings can exhibit the required adhesive strength and RRR. The quality of the sputter coated Cu layers is strongly dependent on the manufacturer and coating parameters.

A procedure for the efficient testing of the Cu coating thickness distribution on the quench heater base material and on the finished heaters, based on 4-point electrical resistance measurements, has been developed. The influence of the electrically conductive 304L steel and interlayer substrate on the Cu coating thickness determination by resistance measurements has been studied and correction factors have been introduced. To evaluate the adhesion of the Cu coating to the 304L surface, a number of adhesion tests have been researched and applied to the Cu coating production samples.

For the 11 T dipole Nb_3Sn HL-LHC magnets interlayer quench heaters are developed that must withstand the $650 \,°C - 50$ h coil reaction heat treatment. In collaboration with the CERN thin film laboratory a study was undertaken to determine the minimum required thickness of an efficient diffusion barrier coating that can prevent Ni diffusion from the substrate into to Cu coating and RRR degradation.

Kurzfassung

Im Rahmen des High Luminosity Upgrade des Large Hadron Collider (HL-LHC), werden neu entwickelte, supraleitende Nb_3Sn Magnete eingebaut. Zum Schutz dieser Magnete werden auf den Magnetspulen so genannte Quenchheizer (QH) installiert. Die Leiterbahnen dieser Quenchheizer werden aus einer Stahlfolie geätzt, welche mit einem Polyimidefilm verklebt ist. Der Prozess ist an die Produktionstechnologie flexibler Leiterplatten angelehnt. Für alle neu eingebauten Magneten werden circa 500 Quenchheizer mit insgesamt 3000 m Laminat benötigt.

Um den elektrischen Widerstand der Leiterbahnen innerhalb der Spezifikationen zu halten, wird vor dem Ätzen auf die Stahlfolie eine ca. 10 µm dicke Kupferschicht appliziert. Die Eigenschaften dieser Kupferbeschichtung sind ein entscheidendes Qualitätsmerkal der Quenchheizer. Der Schwerpunkt dieser Thesis liegt auf der Charakterisierung der Kupferschichten, welche entweder elektrochemisch, durch Sputtern oder durch Elektronenstrahl Verdampfung auf die Stahlfolie aufgebracht werden können.

Die Qualität der Kupferbeschichtungen unterschiedlicher Hersteller wurde durch Widerstandsmessungen bei Raumtemperatur (RT), Ermittlung des Reswiderstands-verhältnisses und durch Adhäsionstests überprüft. Alle hier untersuchten elektrochemisch hergestellten Kupferschichten mit Ni Zwischenschicht haften gut auf der Stahlfolie und haben einen geringen elektrischen Widerstand bei RT und 4.2 K. Die durch Elektronenstrahl Verdampfung hergestellten Schichten können ebenfalls ein gutes Restwiderstandsverhältnis und ausreichend hohe Adhäsion erreichen. Die Qualität der durch Sputtern hergestellten Kupferschichten schwankt stark, je nach Hersteller und Beschichtungsparametern.

Zur Messung der Kupferschicht-Dicke auf dem QH Grundmaterial und den geätzten Quenchheizer Leiterbahnen, wurde eine Messprozedur, basierend auf der Vier-Punkt Widerstandsmessung, entwickelt. Der Einfluss der Stahlfolie und der Nickel Schicht auf die Schichtdickenermittlung durch Widerstandsmessung, wurde untersucht und Korrekturfaktoren wurden eingeführt. Zur Ermittlung der Adhäsion wurden verschiedene Tests angewendet.

Für spezielle Quenchheizer, welche der Nb_3Sn Wärmebehandlung bei 650 °C-50 h standhalten müssen wurde in Zusammenarbeit mit dem Labor für Beschichtungstechnik am CERN eine Kupferbeschichtung mit Diffusionsbarriere entwickelt, welche die Diffusion von Nickel in die Kupferschicht verhindert und damit ein hohes Restwiderstandsverhältnis gewährleistet.

Acknowledgements

Table of Contents

List of Figures

List of Tables

1 Introduction

The Large Hadron Collider (LHC) [1] is the most powerful particle accelerator today. Located at the European Organization for Nuclear Research (CERN) at the Franco/Swiss border near Geneva, it is used to create particle collisions for high energy physics experiments. The particles, hydrogen protons or lead ions, are accelerated and then made to collide in the four interaction regions, where the counter rotating beams intersect. In these collision areas are the four main detectors (ATLAS, ALICE, CMS, LHCb) that collect data from the collisions. The collected data is analysed by physicists at CERN and is distributed to numerous collaborating institutes around the world. Figure 1 shows a schematic view of the CERN accelerator complex with the LHC, and with the numerous particle physics experiments.
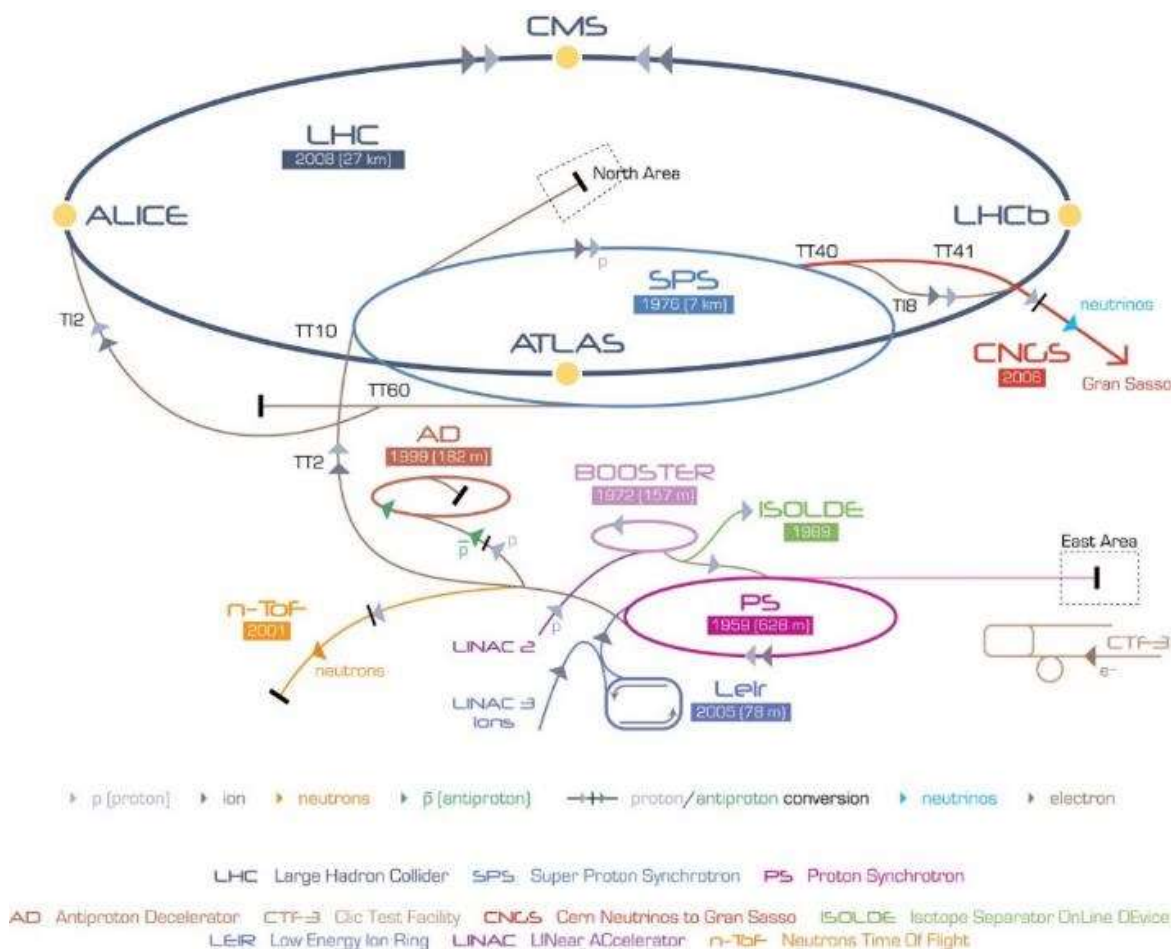
Figure 1: Overview of the CERN accelerator complex and experiments [1].

The LHC relies on superconducting electromagnets [2] for the bending and focusing of the particle beams. In order to increase chances of new discoveries in particle physics, the particle collision rate needs to be increased in the framework of the High Luminosity LHC upgrade (HL-LHC) [3]. This requires a major upgrade on the current machine, which will be fully implemented around 2020.

Figure 2: Cross section of the superconducting dipole magnets in the LHC tunnel [2].

Among other improvements new superconducting magnets [4] will be installed in the LHC. As an example, in order to make room for the additional collimators in the LHC arcs some of the currently installed 9 tesla main dipole magnets (Figure 2), made of Nb-Ti superconductors, need to be replaced with shorter and more powerful 11 T dipoles, using Nb_3Sn superconductors. The 11 T Nb_3Sn dipoles will be integrated in the existing infrastructure, power network and quench protection system of the LHC.

The LHC magnets are operated with up to 12 kA current in the superconducting coils at temperatures of approximately 1.9 K. A beam loss, change in temperature, frictional heat due to mechanical movement or exceeding the critical current can cause the superconductor to transform from superconducting into the resistive state. This transition is called a quench. In order to avoid

---

[2] CERN CDS/Multimedia/Photos (http://cds.cern.ch/record/1741036), 22nd February 2017

the destruction of the magnets due to the resistive heat developing at the high operating currents, a sophisticated quench protection system is required.

The LHC magnet protection system has been developed to protect the magnets in case of a quench and to safely dissipate the energy of approximately 7 MJ stored in the magnet chain. The quench protection system includes the quench detection systems, the quench heaters (QHs) [5] with power supplies and the energy extraction system. In case a quench is detected the current supply is interrupted and the quench heaters are fired to drive the entire coil into resistive state in order to limit the maximum hot spot temperature of the coil to prevent coil damage. The protection diodes divert the current from the quenching magnet into the dump resistors.

The 11 T Nb$_3$Sn dipoles [6] are manufactured at CERN in a wind and react process. The Rutherford-type cable is made of unreacted Nb$_3$Sn wire, and wound to a coil before the Nb$_3$Sn superconducting compound is formed during a coil reaction heat treatment with a peak temperature of 650 °C. All void space in the reacted coil is then impregnated with epoxy resin, so that the brittle Nb$_3$Sn can resist the high stresses under the Lorentz forces during magnet operation. Quench heaters are positioned on the coil outer surface and impregnated together with the coil. The reliability of the quench heater circuits is of utmost importance for the safe operation of the LHC superconducting magnets.

This thesis focuses on the technology and quality assurance of the quench heaters that are developed and produced for the 11 T dipole superconducting Nb$_3$Sn magnets.

2   The LHC and HL-LHC quench heaters

The different magnets installed in the LHC require different quench heaters specially tailored for the magnets characteristics. This chapter focusses on the presently installed dipole QHs for the LHC main dipoles and the QHs under development for the HL-LHC 11 T dipole magnets. Other QHs for quadrupoles and auxiliary superconducting magnets may be based on the same technology, but will not be discussed here.

2.1   The LHC main dipole quench heaters

The present LHC magnet quench heaters are operated using quench heater power supplies, which consist of capacitors with 7.05 mF capacitance [7]. They can provide a stored energy of approximately 3.5 kJ. The same power supplies will be used for the HL-LHC heaters.

As an example, the quench heaters of the LHC main dipole magnets [8,9] consist of two parallel 25±2 µm-thick, 15±1 mm wide stainless steel (304, 316L or equivalent) strips. The steel strips are partially coated with a 4±1 µm thick Cu layer that provides a low resistance parallel current path to lower the overall heater strip resistance of the 14.6 m long heaters. The 120 mm-long uncoated 304L heating stations are alternating with 400 mm-long Cu plated segments. The heater resistance is about 0.35 Ω/m at room temperature.

Figure 3: LHC quench heater terminal with cut-out of the Polyimide coverlay, so the quench heater power supply can be soldered to the heater trace.

Figure 3 shows a LHC main dipole heater terminal. The heater circuits are embedded between two layers of 75 µm-thick Polyimide films, glued together with a 25 µm thick epoxy glue, to electrically insulate the heater from the coil on the inside and from the collars on the outside. The Polyimide insulation has to provide sufficient electrical insulation, but also a high thermal conductivity to allow for a fast heat transfer to the coil. Figure 4 shows a schematic view of a LHC dipole magnet cross section with the heaters installed on the coil outer layer.
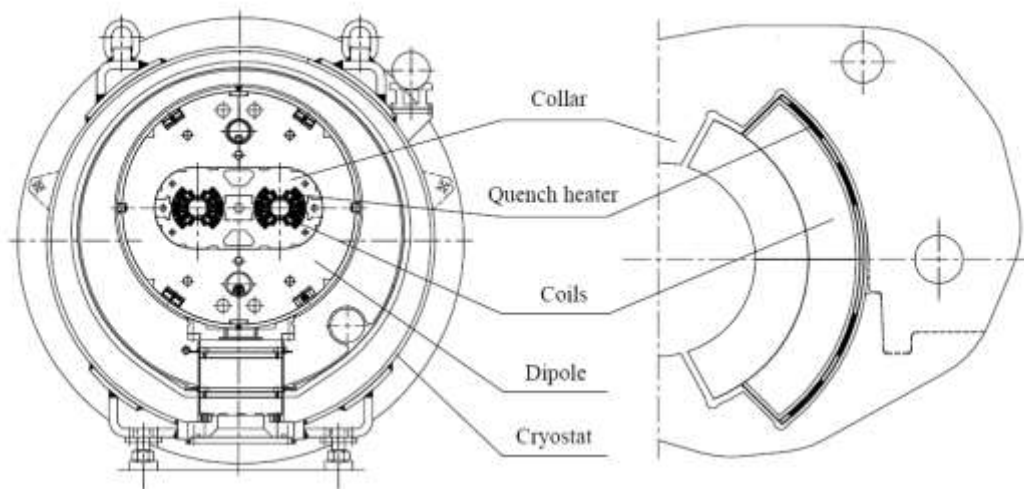
Figure 4: Cross section of a LHC dipole assembly in its cryostat with a detailed view of the quench heater location. (From [9]).

4

2.2   The HL-LHC magnet quench heaters

About 500 quench heaters with lengths varying between 1.5-7.5 m are needed in the coming years for the different Nb$_3$Sn HL-LHC magnets. The heaters need to be impregnated with the coils, and their circuits have comparatively complex shapes, with some of the heater laminates containing additional circuits for voltage measurements and magnet instrumentation. To improve adhesion to the coil, the insulating Polyimide film is perforated with an array of holes.

The QH base material is a laminate consisting of an electrically insulating Polyimide film and a stainless steel foil, onto which a Cu coating is deposited. Just like on the present LHC QHs, the Cu coating of the laminate is needed to reduce the circuit resistance locally by providing a low resistance parallel current path. The heater circuits are etched out of this base material by photolithography. This process is known from Flexible Printed Circuit (FPC) production technology.

The Polyimide film of the QH laminate serves as an electrical insulation between the heater circuits and the coil, but at the same time it has to provide a sufficiently high thermal conductivity to make the QH most effective. To determine the best thermal conductivity with sufficient electrical insulation, different heater-to-coil insulation schemes have been tested in the short model magnets during HL-LHC Nb$_3$Sn magnet development. The best quench heater performance was found, when the quench heaters are impregnated with the coil under a S2-glass sheet [10] as shown for an 11 T dipole coil in Figure 5.
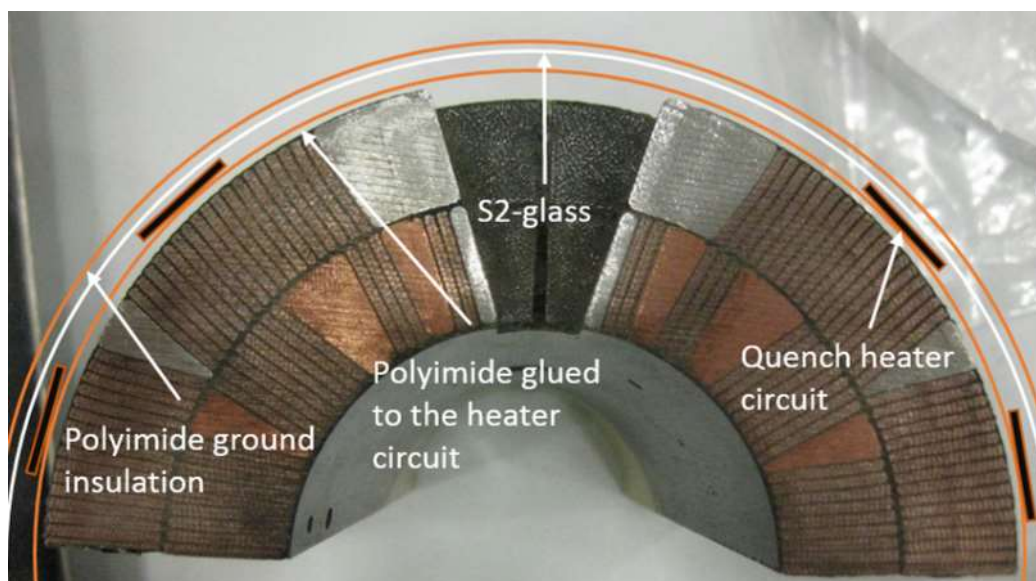
Figure 5: 11 T dipole coil cross section with schematic view of the quench heater insulation scheme.

The insulation of the heater circuit to the collars will be provided by the sheet of S2 glass that is impregnated together with the coil and heater. An additional sheet of Polyimide film is added during coil assembly, to complete the insulation scheme and improve insulation of the heater circuit to the collars. A photograph of the QH impregnated with an 11 T dipole coil is shown in Figure 6.
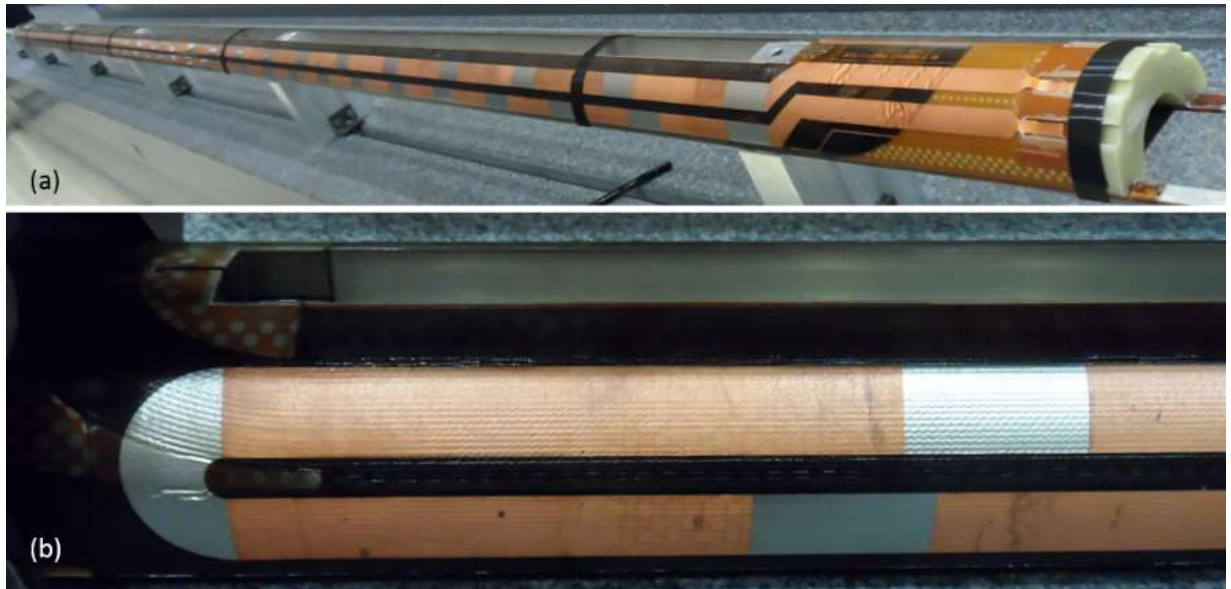
Figure 6: (a) Photograph of a quench heater installed on a 5.5 m long 11 T Nb$_3$Sn coil. (b) Detailed view of the Cu plating pattern and circuit return end.

The maximum resistance of the heater circuits is given by the QH power supply capacitor banks, providing 150 A at 900 V. To keep the overall circuit resistance sufficiently low, the 25 µm-thick 304L steel foil is partially coated with an at least 5 µm-thick Cu layer. In order to serve as an efficient low-resistance parallel current path the Cu coating must have a residual resistivity ratio (RRR) >10.

With the provided power the 11 T dipole heater should reach the designated power density of 90 W/cm^2 in the high-field region, with 25 µm-thick, 50 mm long and 24 mm wide uncoated 304L heating stations, alternated with 130 mm long, 24 mm wide Cu coated regions. In the low-field regions a power density of 145 W/cm^2 is achieved with 50 mm long, 19 mm wide 304L heating stations, alternated with 90 mm long, 19 mm wide Cu coated regions. This Cu plating pattern accommodates for the different speed in quench propagation inside the coil [11]. In this way an overall heater resistance at room temperature below 6 Ω is achieved, including the wiring from power supply to the QH.

2.3   11 T dipole interlayer quench heaters

To reduce the time to quench the entire 11 T Nb_3Sn coils, it is considered to include interlayer quench heaters in the quench protection system. The heaters will be installed between the two coil layers during the winding process. In this layout the quench heaters will be subjected to the 650 °C-50 h coil reaction heat treatment, which requires the heater circuits and insulation to withstand this temperature. To prevent diffusion from steel elements into the Cu layer and to maintain a Cu layer residual resistivity ratio (RRR) >10 it is necessary to develop a coating process that can provide a diffusion barrier between the 304L steel and the Cu coating.

Further an insulation scheme for the interlayer QHs needs to be developed that can resist the HT and provide sufficiently high dielectric properties after impregnation. The Rutherford-type cables for the 11 T coils have an inter-cable insulation consisting of a mica tape and one layer of S2-glass [12]. This insulation scheme is resisting the reaction HT.

3   Quench heater production technology and materials

The HL-LHC quench heaters are produced using Flexible Printed Circuit (FPC) technology [13] in a photolithographic process. The heaters are a composite consisting of an insulating polymer film and the electrically conductive metal foil, which are connected with an adhesive. The electrical circuits are etched out of the laminated metal foil. This chapter gives an overview of the materials commonly used in FPC production.

3.1   Quench heater materials

3.1.1   Film materials

The insulating polymer film between the quench heater circuit and the magnet coil is required to have good dielectric properties to prevent short circuits between coil and heater. On the other hand the thermal conductivity of the film and adhesive should be as high as possible.

Film materials that are commonly used in FPC production are Polyimide (PI), Polyethylene Terephthalate (PET), and Polyethylene Naphthalate (PEN).

PI is the most common film used in FPC production due to its good dielectric strength and its high thermal stability. PI is highly hygroscopic and can rapidly absorb up to 3 % of water from ambient air. [14]

Due to its relatively low cost and good dielectric properties, PET is often used for large-area circuits [15]. PET absorbs less water from the ambient air than PI. The downside of PET is its low thermal stability of 105 °C operating temperature. This requires special procedures for soldered connections on a PET based material.

PEN has a higher thermal stability compared to PET and is therefore used in applications where soldering would damage a PET film. PEN film has a low moisture affinity and good chemical resistance.

3.1.2 Conductor materials

Copper is the most commonly used conductor material in FPC production. Cu has a low electrical resistivity, which allows for highly conductive yet very thin layers. The mechanical properties of Cu are sufficiently good so the conductive film can withstand dynamic stresses of most applications.

Other metal foils that can be used for flexible circuits include stainless steel, nickel-chromium and copper-nickel alloys with high electrical resistance for heater circuits and where corrosion resistance is required [13].

Aluminium is used as conductor material where conductivity is less important but weight reduction and low costs are predominant. Special alloys such as copper-beryllium or phosphor-bronze offer high elasticity (spring like properties) and corrosion resistance paired with a higher conductivity compared to steel. If necessary noble metals like gold and silver can be used [13].

3.1.3 Adhesives used in FPC production

The flexible adhesives needed to bond the electrically conductive metal foil to the electrically insulating film have to be compatible with the film and conductor materials. The adhesive is usually applied to the dielectric film and then joined with the conductive foil in a lamination process. In most cases a heat treatment is required to fully cure the adhesive. Furthermore the adhesive has to be resistant to chemicals to withstand the conditions in the production steps following the lamination. The thickness of the adhesive layer can be influenced for instance by varying the adhesive viscosity and by the duration the film is immersed in the epoxy bath.

Epoxy based flexible adhesive systems are most commonly used in FPC and Printed Circuit Board (PCB) production. Epoxy adhesives have a relatively good temperature resistance, compatible with common soft soldering, they retain flexibility after curing. The properties of the epoxy resin can be

altered with fillers and additives, for instance for flame retardants or enhanced thermal conductivity [15].

Acrylic based adhesives are often applied to PI films and used with metal foils such as stainless steel or nickel alloys. Acrylic adhesives retain good flexibility and chemically resistant, however their temperature resistance is typically lower than that of epoxy based resins. Acrylic adhesives are subject to hydrolysis and high thermal expansion which can cause problems during production and operation.

PET films are often laminated with polyester/polyurethane (PU) adhesives. The downside of PU adhesives is their highly hygroscopic nature, and that they have a lower thermal stability than epoxy based adhesives.

3.1.4 The GTS L960461 Polyimide-304L steel foil laminate

The laminate L960461 produced by GTS Flexible Materials Ltd. consists of a 50 µm-thick Polyimide film, Kaneka Apical AV [14], 15 µm-thick epoxy adhesive (GTS AS1084) and a 25 µm-thick 304L stainless steel foil (hard temper). The epoxy adhesive is cured during a 120 °C-5 h heat treatment in ambient air.

The laminate is produced from 630 mm-wide Polyimide film and steel foil. Afterwards the laminate edges are trimmed to remove excess adhesive and define final dimensions. The laminate width after trimming is 610 mm, which is a standard width in FPC technology. Any other laminate width <610 mm can be supplied by GTS.

According to GTS the laminate can withstand temperatures up to 288 °C for 10 seconds in a soldering process, when pre-dried at 150 °C for 30 minutes. Without pre-drying the laminate, blisters will occur at 250 °C for 10 seconds.

As a reference the 280 mm-wide GTS L960461 laminate (IP number 178910) has been characterised. The laminate thickness measured with a micrometre screw is 90.6 µm ± 1.4 µm. The detached steel foil thickness measured with a micrometre is 25.8 ± 0.9 µm. Residual epoxy adhesive has been removed prior to the measurements. A 304L foil thickness of 24 µm ± 0.2 µm was determined by electrical resistance measurements, assuming a foil resistivity of ρ_{304L}=0.73 Ωmm^2/m at 293 K. The RRR of the 304L foil is 1.3. The measured laminate dimensions correspond with the manufacturer specification.

3.2 The Cu coating of the 304L steel foil

In order to keep the overall heater circuit resistance of the long HL-LHC heaters in acceptable limits (Resistance at RT<6Ω), the stainless steel circuits are coated with a Cu layer that provides a parallel current path on selected heater regions. Main requirements of the Cu coating are a good adhesion to the steel circuit during assembly and during the entire magnet operation, a thickness between 5-10 µm and a RRR≥10. The Cu coating can be applied for instance by electrolytic deposition, or by a physical vapour deposition (PVD) process, for instance electron beam evaporation or sputtering.

3.2.1 Electrolytic Cu deposition

In the electrolytic deposition coating process the substrate and coating material are immersed in an electrolyte that contains ions to permit the flow of electricity between the substrate and coating material. The coating material serves as the anode and the substrate serves as the cathode. Electrical current rapidly oxidizes the anode and the metal atoms from the coating material are dissolved in the solution. At the cathode the metal ions are reduced and form the coating on the substrate. Figure 7 shows a schematic of the process.
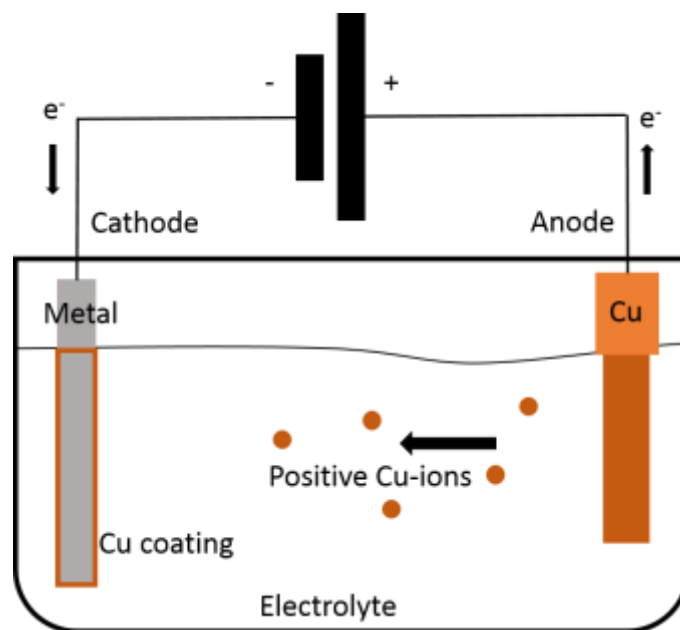
Figure 7: Schematic of the electroplating process. The electrolyte rapidly oxidizes the Cu and the positive Cu-ions are attracted to the negative potential on the cathode.

At the CERN PCB laboratory the Cu coating on the Polyimide 304L laminate is produced in an electrolytic deposition roll-to-roll process to produce sufficiently long laminates for the quench heaters. The machine is shown in Figure 8.

The substrate passes through multiple rollers to expose a large surface area to the electrolyte. The rollers also provide electrical contact to the 304L side of the substrate (Figure 8b).
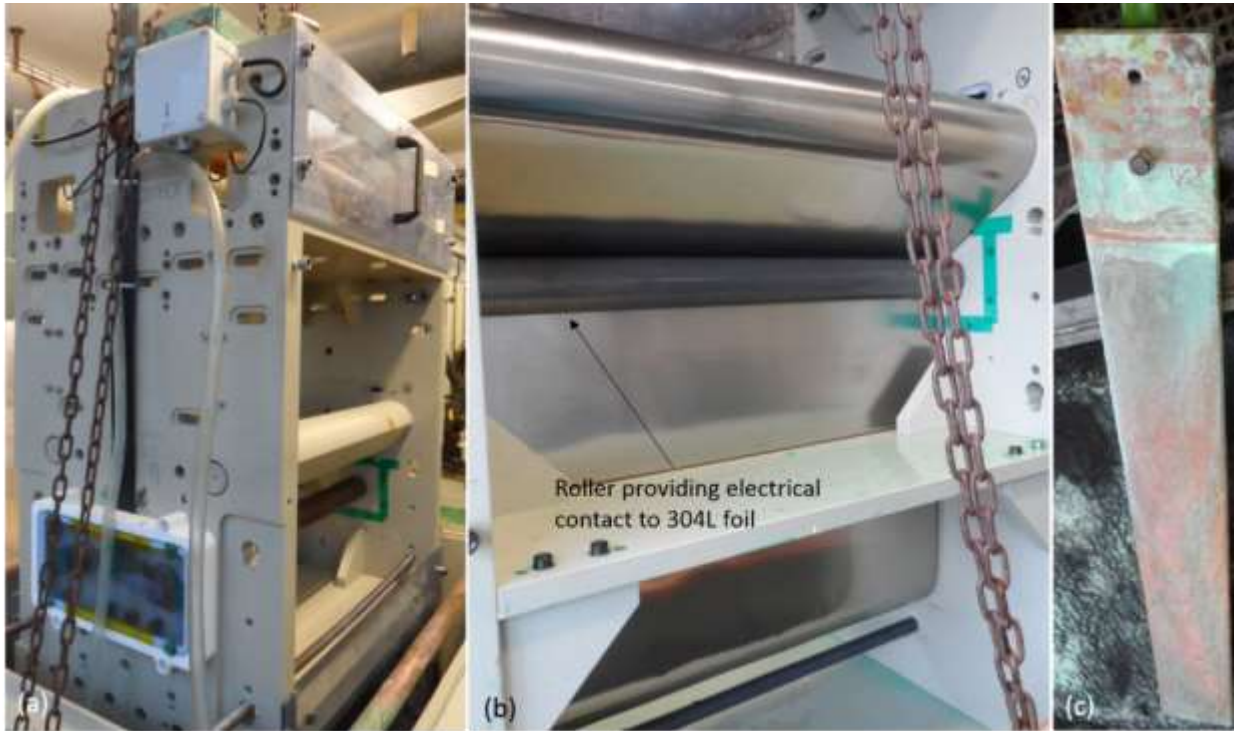
Figure 8: (a) Roll-to-roll coating machine in the CERN PCB laboratory. (b) The Polyimide 304L substrate mounted in the machine with a roller to ensure electrical contact. (c) The Cu electrode, cleaned before the Cu coating process.

Prior to the deposition of the approximately 10 µm-thick Cu coatings, the 304L steel substrate is activated in a $NiCl_2$ - H_2O/HCL solution (Ni 74g/l, HCL 50 ml/l). In the second substrate pass, a Ni layer is deposited to improve adhesion of the Cu coating (Wood's Ni-strike). Ni electrodes are immersed in the above mentioned solution and a current of approximately 150A at 9 V is applied to the substrate and Ni electrodes. After the Ni treatment the laminate is thoroughly rinsed with water to remove residuals from the $NiCl_2$ – H_2O/HCL solution. The Cu deposition is performed with pure Cu electrodes (Figure 8c) immersed with the Laminate in a $CuSo_4$ - H_2O bath (H_2So_4 100 ml/l, Cl 0.075 g/l). The electrolyte is constantly mixed while the plating process is performed at a current of 100 A at 3 V. Four to five roll-to-roll passes of the laminate are needed to achieve the 10 µm thick Cu coating. When the coating process is finished the laminate is rinsed with water and dried with compressed air. Figure 9a shows the Cu coated laminate just after production. In ambient air the Cu surface oxidises almost instantly after the process (Figure 9b).
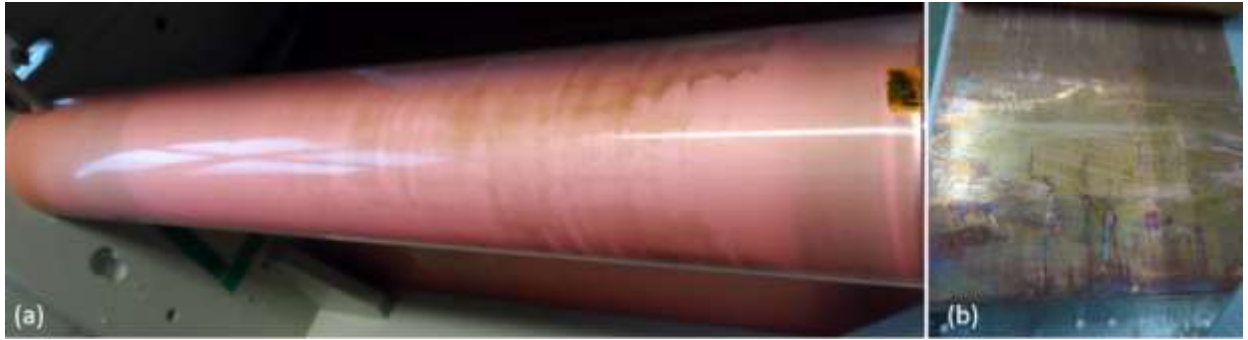
Figure 9: (a) The Polyimide 304L laminate after the Cu coating process still in the machine. (b) The Cu surface oxidises after a short time exposed to ambient air.

3.2.2 Electron beam evaporation

The Physical Vapour Deposition (PVD) processes sputtering and electron beam evaporation are alternative processes to produce the Cu coating. Both can be conducted in a roll-to-roll process and could be suitable to produce sufficiently long laminate for the quench heaters. Electron beam evaporation could be potentially faster than the electrolytic deposition at CERN's PCB laboratory.

In the PVD process Cu is evaporated by a directed high energy electron beam (E-beam) and deposited on the substrate. The steel 304L surface can be pre-treated with ion sputtering to clean the substrate and enhance surface energy for better adhesion. Furthermore thin matching layers can be deposited before application of the final Cu layer. A schematic of the different in-line process steps that can be performed with modern coating machines is shown in Figure 10 [16].
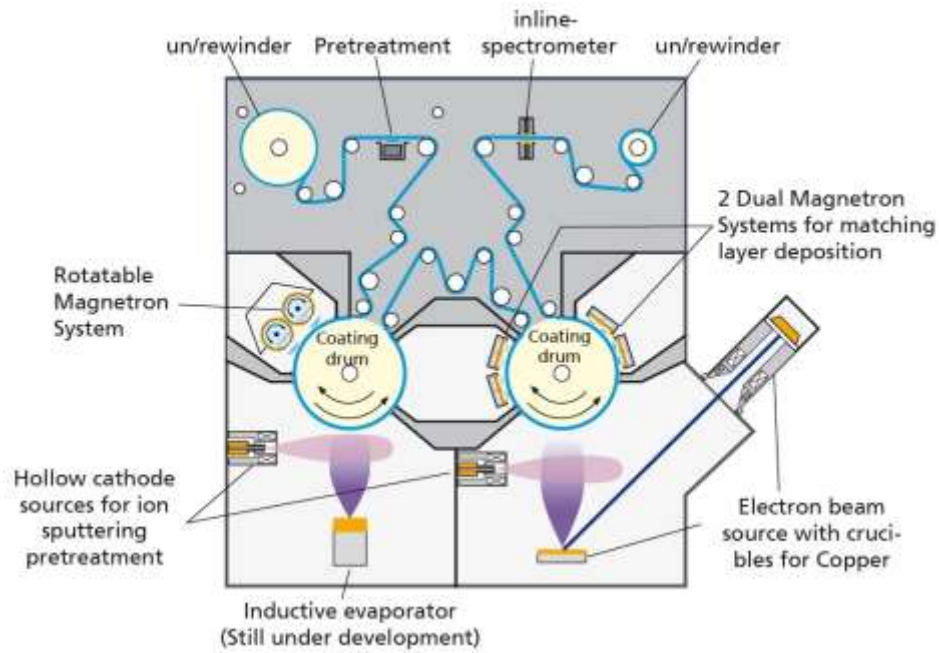
Figure 10: Schematic of the "novoFlex®600" roll-to-roll pilot web coater used at Fraunhofer FEP for the coating of up to 600 mm wide substrates on rolls with a diameter of up to 500 mm. All process steps can be performed in-line without exposing the substrate to ambient air [16].

One of the challenges in PVD processes can be the high substrate temperature that can occur in a high deposition rate process. In case of the GTS Polyimide-304L laminate, temperatures over 260 °C degrade the adhesion of the laminate and can cause blistering of the laminate. The temperature resistance of the laminate can be somewhat improved when it is dried in vacuum or inert gas at temperatures up to 150 °C. In addition a multi-pass Cu coating process can be performed in order to limit the heat exposure during layer deposition, which results in increased process times. An alternative approach is the Cu deposition on a 304L foil that is then laminated to the Polyimide film after the coating process.

3.3 Photolithographic etching of the heater circuits

The quench heater circuits are etched out of the Cu coated Polyimide-304L laminate in a selective etching process. A possible production sequence is listed below:

- To ensure proper alignment of the laminate during the following process steps a series of alignment holes is drilled.

- The whole substrate is then chemically cleaned.

- A dry film photoresist is laminated onto the cleaned Cu surface of the QH laminate.

- The dry film above the QH circuit is then cured by laser direct imaging or using a mask, in order to produce an etchant resistant coating.

- In a developer solution the unexposed dry film is removed, leaving the uncovered Cu surface.

- In the subsequent etching process the Cu coated 304L foil is completely removed in all areas that are not covered by the cured photoresist.

- The photoresist is removed from the QH circuits.

- The circuit is chemically cleaned.

- The steps are repeated to remove the Cu coating on the 304L heating stations.

The laminate exposure in the acid bath should be limited in order to avoid a strong degradation of the epoxy adhesive between the Polyimide film and 304L foil. Such a degradation has for instance been observed on the heater circuits T8000003 and T8000004 (see Figure 12 below).

As the last heater production step, holes are drilled in the Polyimide film to improve adhesion of the heater during the magnet coil impregnation process. Several heater circuits can be etched from a 600 mm-wide laminate and prior to installation the excess Polyimide film is removed so the heater fits the coil outer shape.

4 Quench heater quality control tests

4.1 Visual heater inspection

Upon reception at CERN all quench heaters are visually inspected for obvious signs of defects to the Polyimide-304L laminate and the Cu coating. Figure 11 shows examples of the inspected quench heater circuits for dipoles.

Figure 11: (a) Visual inspection of the QH T8000005/006 without large visible defects. (b,c) Delamination of the 304L foil from Polyimide film and thick oxide scale on the Cu coating of the heaters T8000003/004.

Visual inspection of the laminate and Cu coating of the heaters T8000003 and T8000004 revealed very low adhesion between the 304L foil and Polyimide film, presumably due to prolonged exposure to the etchant. The Cu coatings are severely oxidised (Figure 12). In addition in QH T8000003 an impurity was found between the 304L foil and Polyimide film (Figure 12a) that could have damaged the Polyimide film if the heater would have been installed in a magnet.

Figure 12: Heater circuit T8000003 and T8000004. (a) Inclusion between Polyimide film and 304L foil that may damage the Polyimide insulation. (b and c) Partially delaminated circuits.

4.2 RT heater circuit resistance measurement

The room temperature (RT) electrical resistance of the quench heater circuits is measured with the four-point method using a Digital Low Resistance Ohmmeter "Megger DLRO10" (Figure 13). Resistance measurement results that have been obtained for several 11 T dipole QH circuits are summarised in Table 1.

Figure 13: four-point resistance measurement of a quench heater circuit before impregnation with DLRO 10 handspikes.

Resistance measurements have been taken before, and after the coil impregnation process for the QH circuits that where installed on magnet coils. The Cu pattern at the return of the heater circuits T8000001 and T8000002 (See Figure 6b) does not correspond with the production drawings. The effect of the altered Cu plating pattern appears to be negligible for the overall circuit resistance.

16

On the QHs with reference numbers T8000003 and T8000004 the resistance of both heater circuits has been measured and the oxidised Cu coating does not seem to have an effect on the circuit's resistance.

Table 1: Resistance of different 11 T dipole quench heater circuits before and after impregnation with the respective coil. Measurements were taken at RT with 1 mA current (Average resistance over 3 measurements).

	Before impregnation	**Resistance (Ω)**
T8000001	LH-circuit	5.596±0.001
	RH-circuit	5.650±0.001
	After Impregnation with coil CR000001	
	LH-circuit	5.599±0.002
	RH-circuit	5.6503±0.001
T8000002	**After Impregnation with coil CR000002**	
	LH-circuit	5.605±0.0006
	RH-circuit	5.573±0.0006
T8000003	**Before impregnation**	
	LH-circuit	5.573±0.0006
	RH-circuit	5.606±0
	Before impregnation	
	LH-circuit	5.513±0
	RH-circuit	5.473±0
T8000004		
	After Impregnation with coil CR000003	
	LH-circuit	5.539±0.004
	RH-circuit	5.567±0.001
T8000005	**Before impregnation**	
	LH-circuit	5.740±0.0006
	RH-circuit	5.747±0.001
T8000006	**Before impregnation**	
	LH-circuit	5.824±0.001
	RH-circuit	5.721±0.001

For comparison a heater circuit resistance of 5.3 Ω has been estimated using the dimensions given in the production drawing (Appendix 2), assuming a resistivity for the stainless steel and pure copper of $\rho_{304L} = 0.73$ $\Omega mm^2/m$ and $\rho_{Cu} = 17.2 \cdot 10^{-3}$ $\Omega mm^2/m$, respectively. The copper coated 304L

segments have been modelled as two resistors connected in parallel, with the interlayers not considered. The calculated resistance of the different heater segments is shown in Table 2.

Table 2: Circuit resistance calculated from the theoretical resistance of the different quench heater circuit segments. The heater geometry is based on the heater drawing shown in Appendix 2.

Material and dimensions	Number of segments	Resistance (Ω)
304L 25 µm×19 mm×50 mm (uncoated)	37	2.93
304L 25 µm×24 mm×50 mm (uncoated)	29	1.82
304L 25 µm+10 µm Cu, 19 mm×90 mm	36	0.28
304L 25 µm+10 µm Cu, 24 mm×130 mm	28	0.25
End semi-circle radius 17 mm, length 52 mm, width 21.5 mm, 304L+10 µm Cu	1	0.004
Connection width 19 mm, medium length 235 mm 304L+10 µm Cu	2	0.02
Total circuit resistance		**5.33**

4.3 Measurement of the Polyimide film dielectric properties

The integrity of the Polyimide electrical insulation is needed to prevent short circuits between the magnet coils and heater circuits, which is crucial for the safe operation of the HL-LHC magnets. Therefore the dielectric strength of the finished QH is tested before installation. The high voltage and leakage current test procedure for the HL-LHC heater remains to be defined. A possible set-up that was used for the LHC QH with Polyimide insulation on either side of the heater is shown in Figure 14.
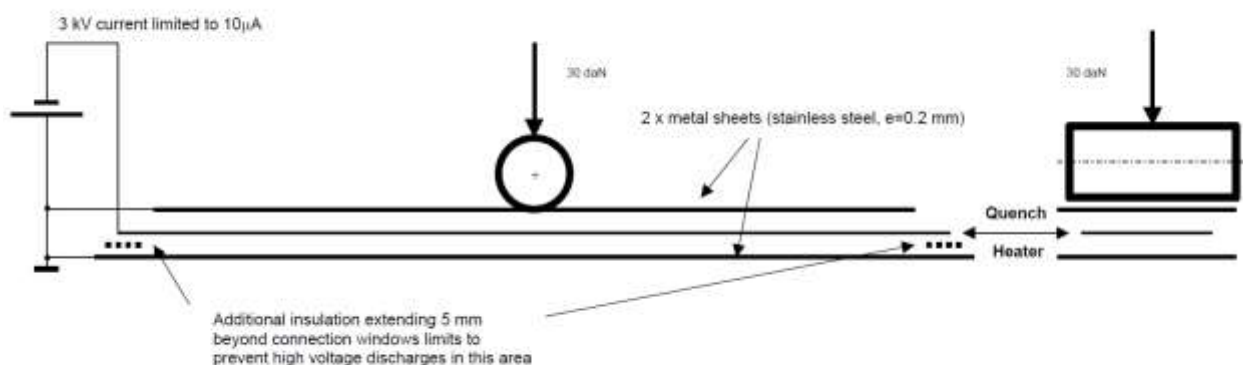
Figure 14: Schematic of a high voltage test set-up for LHC QH quality control. Reproduced from [8].

For the HL-LHC QHs without a coverlay the test set-up shown in Figure 15 can be used. The Polyimide side of the QH is placed on a 2 m-long flat Cu surface, and additional weight is placed on top of the QH to ensure good contact between the flexible laminate and the Cu surface. An insulation tester Megger S1-1054/2 is connected to the QH terminals and the Cu surface. A voltage of 3 kV is applied for a time period of 30 seconds during which the resistance is constantly monitored. For the 5.5 m long 11 T dipole heaters three measurements along the QH laminate are needed due to the limited setup length. The leakage current rate has been calculated from the applied voltage and the measured resistance.

Figure 15: (a) The Megger S1-1054/2 insulation tester used for the dielectric measurements. (b) Connection of the tester to the QH terminals. (c) The test setup with additional weights.

The quench heaters QH_11T_Tr_002 and QH_11T_He_001, the later consisting of Polyimide film and 304L foil only, have been tested with this setup and results are shown in Table 3. On the QH_11T_Tr_001 circuit, one defect was found as shown in Figure 16. The small hole in the Polyimide film caused a short circuit from the QH 304L foil to the Cu plate.

Figure 16: Perforated Polyimide film below the QH circuit that was detected during a HV test.

After application of additional Polyimide tape in the perforated area no further defects where found. The different resistance and leakage currents found for both heaters may be partly attributable to the different etching procedures.

Table 3: Results of the room temperature dielectric measurements at 3 kV (average of three measurements over the circuit length, test duration 30 seconds).

	Leakage current (nA)	Resistance (GΩ)
QH_11T_Tr_002	157±9.0	19.2±1.1
QH_11T_He_001	302±26	10.0±0.9

Further dielectric tests have been performed on full length QH circuits T8000005 and T8000006. Results are shown in Table 4. The measurements have been performed with the QH placed on an aluminium foil and additional load on top to ensure good contact between the Polyimide film and the aluminium foil. In this test the leakage current was measured and the resistance is calculated form the measurement results and applied voltage.

Table 4: Test of the Polyimide dielectric strength on the QH circuits T8000005/006. Test voltage 5 kV applied for 2 minutes with a Megger S1-5010 insulation tester.

	Leakage current (nA)	Resistance (GΩ)
T8000005	519	9.64
T8000006	432	11.58

4.4   Measurement of the quench heater and circuit dimensions

The circuit dimensions and the Cu pattern will be verified using a template. The allowable geometrical deviations of the heater circuit and pattern from the production drawing are to be defined. The distance of the holes in the Polyimide to the circuit and to the Polyimide film edges must be at least 4 mm to ensure the dielectric strength of the Polyimide film.

4.5   Cu coating thickness measurements

Four different Cu coating thickness measurement methods have been in order to select a reliable and efficient technique for future routine quality controls of the Cu coated QH base material [17]. Additional Cu thickness measurement methods that have been considered but not been applied to the samples are listed in Appendix 6.

4.5.1   Thickness measurements in FIB coating cross sections

The Cu coatings of the QH laminates have been characterised by Scanning Electron Microscopy of coating cross sections that have been prepared by Focused Ion Beam milling (FIB-SEM). The FIB-SEM cross sectional image of an electrolytic Cu coating is presented in Figure 17 and the thickness results that are derived from two FIB-SEM images are summarised in Table 5. These thickness measurement results can be compared to the thicknesses measured with a micrometre gauge, and those derived from electrical resistance measurements, which are presented below.
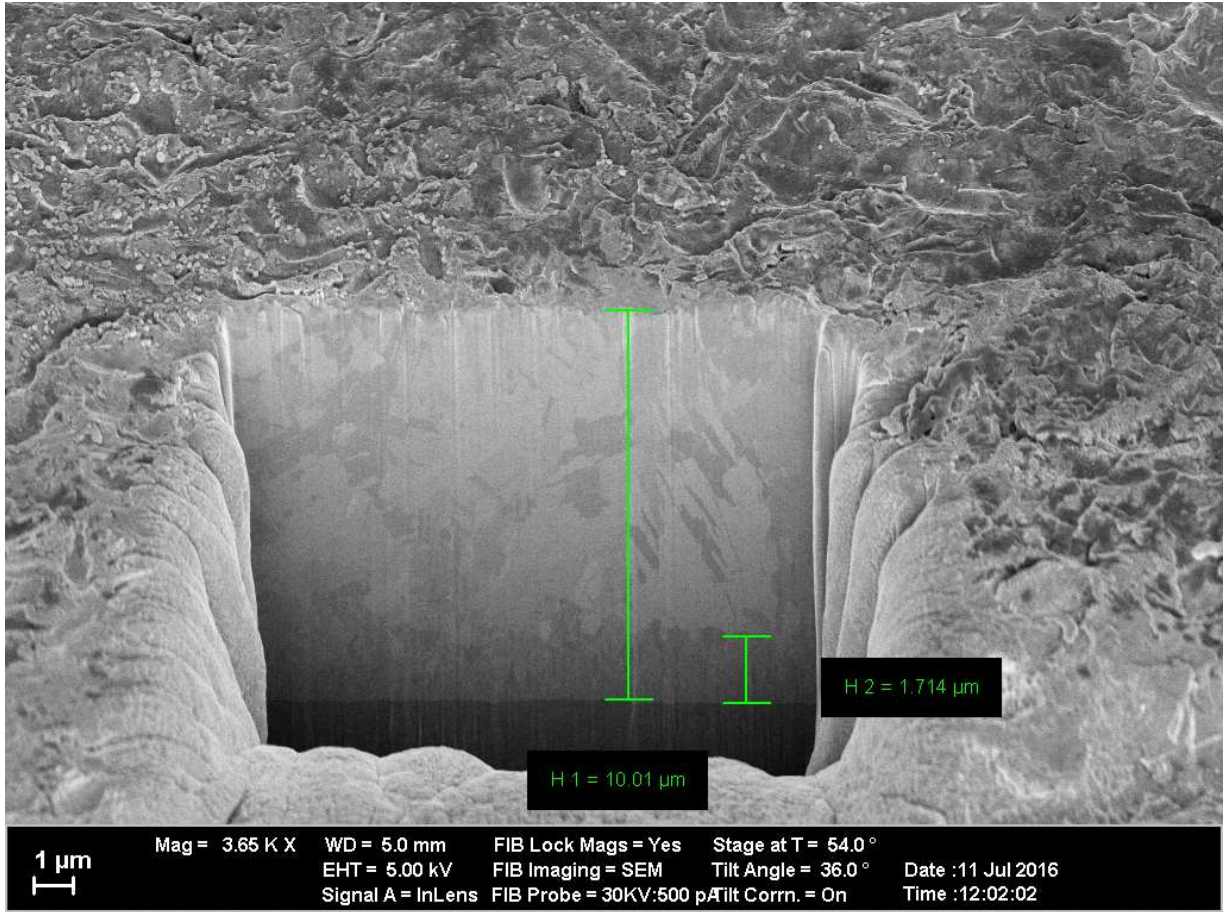
Figure 17: FIB-SEM cross sections of an electrodeposited Cu coating with Ni interlayer. Courtesy M. Hagner, University of Konstanz.

Table 5: Cu coating and interlayer thickness measured in FIB-SEM cross section.

Supplier and coating method	Thickness (µm)		
	Cu	Interlayer	Total
CERN PCB lab; electrolytic	8.3	1.7	10.0
E-beam evaporation (2016-08-10A)	6.6	0.2	6.8

4.5.2 Thickness measurement with micrometre gauge

Thickness measurements of the 304L steel-Polyimide laminate and of the detached steel foil with and without Cu coating have been performed with a micrometre gauge with a measurement range of 0 to 25 mm (Figure 18). According to [18] the micrometre gauge measurement uncertainty is ±2 µm.

Figure 18: Measurement of the stainless steel foil thickness with a Tesamaster micrometre.

The laminate (IP number 178910) has a thickness of 90.6±1.4 µm. For the measurements the 304L foil has been detached from the Polyimide film and cleaned from residual epoxy adhesive. The delaminated steel foil has a thickness of 25.8±0.9 µm (Table 6), which is in good agreement with the respective nominal values of 90 µm and 25 µm given by the manufacturer.

Table 6: Micrometre gauge thickness results of Polyimide-steel laminate and its disconnected steel foil (average values of eight thickness measurements ±1 σ).

	Thickness (µm)
Polyimide 304L laminate	90.6±1.4
304L foil	25.8±0.9

In order to derive the Cu coating thickness, the thickness of the uncoated foil (25.8 µm) is subtracted from Cu coated steel foil thickness. The difference between the Cu coating thickness derived from micrometre measurements and by FIB-SEM (Table 7) is presumably credited to the uncertainty of the micrometre thickness measurements.

Table 7: Micrometre gauge thickness results of Cu coated 304L steel foils (average values of eight thickness measurements ±1 σ) and the Cu coating thickness derived as the difference between the coated and uncoated steel foil. The coating thickness measured by FEB-SEM is shown for comparison.

	Micrometre (µm)		FIB-SEM (µm)
	Cu coated 304L	Cu and interlayer	Cu and interlayer
CERN PCB lab; electrolytic	38.6±1.3	12.9±1.2	10.0
E-beam evaporation (2016-08-10A)	36.4±1.3	10.6±1.3	6.8

4.5.3 Cu coating thickness determination by surface resistance measurements

The thickness of metallic coatings on insulating materials can be calculated from the coating surface resistance when the resistivity of the coating at the test temperature is known. Measurements are based on the procedure "Measurement of coating thickness – Microresistivity method", as specified in EN 14571 [19]. This procedure is applicable to the thickness measurement of one electrically conductive coating on top of an electrically insulating substrate. In contrast, the quench heater Cu coating is deposited onto a stainless steel substrate, with an interlayer made for instance out of Ni. The electrical conductivity of these layers causes an uncertainty in the Cu layer thickness measurement. To evaluate the influence of the electrically conducting substrate materials on the surface resistance, the heater circuit is modelled as three resistors connected in parallel (Figure 19).
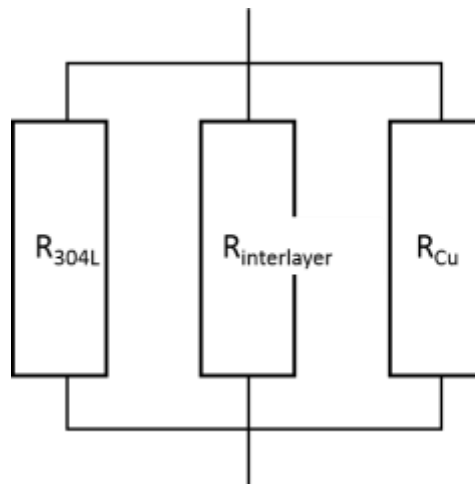
Figure 19: Cu coated 304L steel strip with interlayer modelled as three parallel resistors.

The electrical resistivity, and calculated resistances of the metallic heater layers is summarized in Table 8. Exemplary for interlayers that can be used in the coating process, the resistance of a NiCr8020, Ni and a Ta interlayer is calculated. The resistance is calculated for 2 mm-wide and 100 mm-long strips, which is also the sample geometry used for RRR measurements.

Table 8: RT resistance of the different QH layers (R_i) calculated from the coating cross sections (A) and electrical resistivity (ρ), (100 mm voltage tap distance, 2 mm width).

Material	Thickness [mm]	A [mm^2]	ρ at 293 K [Ωmm^2/m]	R_i [Ω]
Copper	5.0 10^{-3}	0.010	0.017 [20]	0.17
NiCr8020	0.20 10^{-3}	0.0004	1.08 [21]	270
Ni	1.0 10^{-3}	0.002	0.061 [20]	3.1
Tantalum	0.20 10^{-3}	0.0004	0.13 [20]	33
304L stainless steel	25 10^{-3}	0.050	0.73 [22]	1.5

The electrical conductivity of the 25 µm-thick steel foil and the 1 µm-thick Ni interlayer that is deposited before electrolytic Cu coating causes a significant error in the determination of the QH Cu coating thickness based on the surface resistance measurements according to EN 14571. As an example, the electrical resistance of a 5 µm thick Cu layer on a 25 µm-thick steel foil is 10% lower, compared to a 5 µm thick Cu layer deposited onto an electrically insulating film, and the Cu coating thickness is overestimated as shown in Figure 20a. The relative Cu thickness error caused by the electrically conducting substrate materials is presented in Figure 20b as a function of the true Cu thickness.
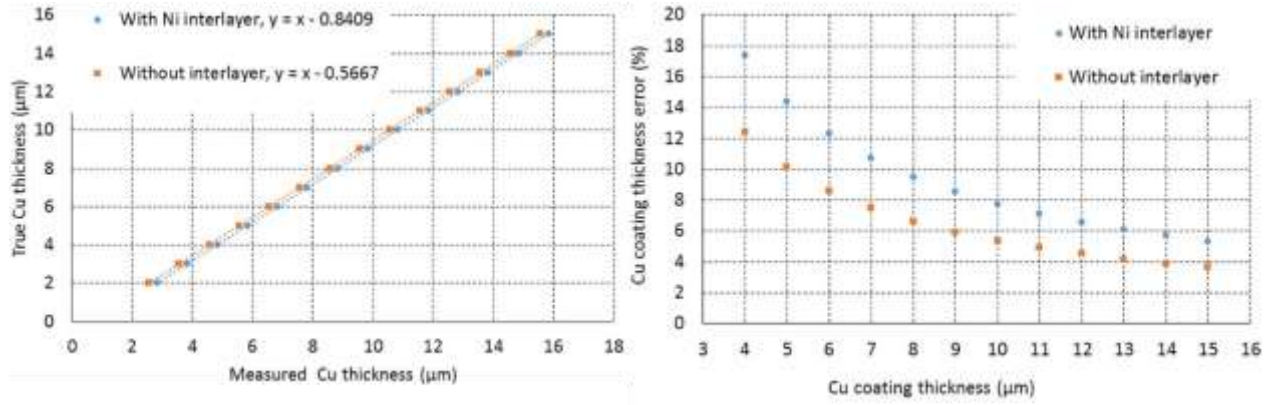
Figure 20: (a) True Cu thickness vs. the measured Cu thickness. (b) Relative error of the Cu thickness derived from electrical resistance measurements due to the electrically conducting 25 μm-thick steel foil as a function of the Cu coating thickness. For electrolytic Cu coatings a 1 μm-thick Ni interlayer further reduces the surface resistance, causing an additional error in the Cu coating thickness determination.

With Equation 1 for a Cu coating with Ni interlayer and Equation 2 for a Cu coating on 304L, derived from the plot in Figure 20a the real Cu coating thickness can be calculated from the measured Cu coating thicknesses.

Equation 1: $$t_{Cu\ real} = t_{Cu304\ Ni\ intlayr} - 0.841$$

Equation 2: $$t_{Cu\ real} = t_{Cu304} - 0.567$$

➢ *Surface resistance measurements with a Digital Low Resistance Ohmmeter*

Four-point resistance measurements are performed with a Digital Low Resistance Ohmmeter (Megger DLRO10X) [23]. The set-up with duplex hand spikes that hold the current injector pins and voltage taps is shown in Figure 21. A test current of 100 mA is injected in a distance of 5 mm from the voltage taps. The accuracy of the inhomogeneous current distribution due to the point like current injection close to the voltage taps causes a systematic error in the resistance results. A minimum distance between the voltage taps and defined sample geometry is needed to obtain representative results. Multiple sample geometries with varying voltage taps distances have been tested and the sample geometry described below proved to deliver representative results.

Figure 21: Four-point resistance measurement of a 10 mm wide, 160 mm long Cu coated sample, using a DLRO-10 with duplex handspikes.

Resistance at ambient temperature (RT) has been measured with voltage tap distances ranging from 1 cm to 16 cm on 1 cm wide strips, cut from the Cu coated laminate. At each voltage tap distance three measurements have been acquired. The Cu coating thickness t (in cm) is then calculated with Equation 3 (Cu resistivity at RT ρ_{Cu} =1.72 10^{-6} Ωcm, distance between voltage taps *l* in cm, resistance *R* in Ω, sample width *w* in cm).

$$\text{Equation 3:} \qquad t = \frac{\rho_{Cu}\, l}{R\, w}$$

> ➤ *Thickness measurements with Fischer SR-Scope*

The Fischer SR-SCOPE RMP30-S tester (Figure 22) is dedicated for the measurement of copper coating thickness on Printed Circuit Boards [24], according to EN 14571 [19]. The tester was calibrated with the ERCU N four-point probe and three standard samples provided by the manufacturer (17.0 µm and 64.9 µm-thick Cu coatings deposited onto insulating fiberglass laminate, and a pure Cu reference sample). The voltage taps of the Fischer ERCU N 4-point probe

have a pre-set distance and the thickness of the conductive coating is calculated internally and displayed on the SR Scope. The operator can choose between two Cu thickness measurement ranges (0.1 to 10 µm, or 5 to 120 µm). The measurement repeatability precision stated by the manufacturer is 0.2 µm ≤ s ≤ 2%.

Figure 22: Cu coating thickness measurements with the Fischer SR-Scope RMP30-S tester in combination with the Fischer ERCU N four point probe.

The results of different Cu coating thickness measurements acquired with the Fischer SR-Scope, the DLRO10, the micrometre gauge and in FIB-SEM cross-sections are compared in Table 9. As outlined above, due to the presence of the electrically conducting steel foil the electrical resistance measurements overestimate the Cu coating thickness by about 10%. This error is not considered.

*Table 9: Comparison of the Cu coating thicknesses measured with four different methods. *Without interlayer. **With interlayer.*

Coating method		Thickness (µm)			
		DLRO 10	Fischer SR-Scope	FIB-SEM cross section*	Micrometre measurements**
CERN PCB lab; electrolytic		9.2±0.05	9.6±0.2	8.3	12.9±1.2
CERN TE-VSC; sputtering	100nm Ta	6.0±0.4	6.1±0.6	5.2	4.9±1.5
	200nm Ta	6.8±0.3	6.3±0.8	5.8	6.6±1.2
	100nm Mo	6.1±0.3	6.1±0.9	5.5	5.9±1.2
	200nm Mo	6.5±0.2	6.0±1.1	6.4	6.1±1.2
E-beam evaporation (2016-08-10A)		6.6±0.1	6.1±0.5	6.6	10.6±1.3

Reasonably good agreement is found between the electrical (DLRO 10 and Fischer SR-Scope) and the FIB-SEM coating thickness results. The relatively strong deviation of the micrometre thickness results of some coatings can be partly attributed to the measurement uncertainty of the micrometre measurements. In the case of the CERN PCB coating the 1.7 µm-thick Ni interlayer also contributes to the thickness difference observed with the different methods.

Since the non-destructive Fischer SR-Scope thickness measurements are reliable, and their acquisition is much faster as compared to the other methods, these tests are now performed for the routine QC of the Cu coated QH base material.

4.5.4 Cu coating thickness distribution on 610 mm-wide and up to 7.5m-long steel-Polyimide laminate

The thickness distribution of the electrolytic Cu coating has been measured on four 610 mm-wide steel-Polyimide laminates with 5.5 m or 7.5 m usable length. The coatings were produced at the CERN PCB laboratory between November 2016 and January 2017.

Figure 23 shows the QH substrate 5.5m_001 with 5.5m usable length. The total length of the laminate is 7.5 m, and on each side up to 1 m laminate is not homogeneously coated and needs to be removed (Figure 23d). The Cu coating shows a heavily oxidised surface appearance and in some

areas a rough surface structure. The outermost layer can be partly removed after the circuit etching process, and is not supposed to have a strong influence on the Cu coating electrical properties. At the laminate edges the Cu coated 304L steel foil is partially delaminated from the Polyimide film (Figure 23b). This is a result of the foil misalignment in the reel-to-reel coating machine, and about 1 cm on either side of the Cu coated laminate needs to be removed.
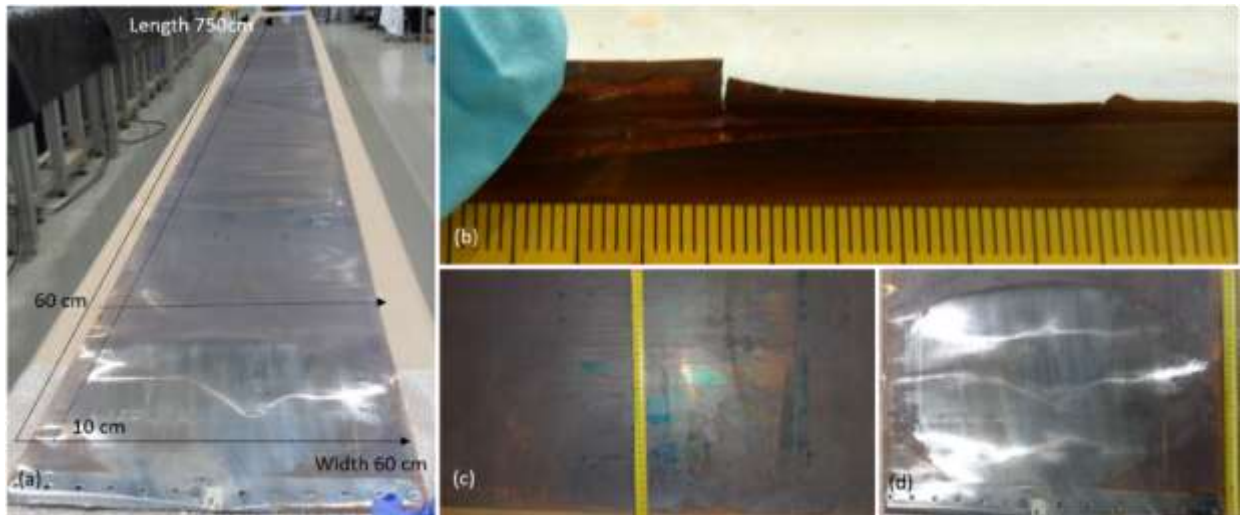
Figure 23: (a) Visual appearance of the Cu coating and measurement reference coordinates of the 5.5m usable QH substrate. (b) Partially delaminated regions at the outermost laminate edges need to be removed. (c) Appearance of usable Cu coating. (d) On this laminate the first approximately 0-0.6 m and the last 7.0-7.5 m of the substrate are not well coated and need to be removed.

The Cu coating thickness was measured with the Fischer SR-Scope, set to a measurement range of 5-120 µm, in combination with the Fischer ERCU N 4-point probe (Figure 22). The calibration was performed at ambient temperature using the calibration standards described above. Before the thickness measurements all laminates have been acclimatized for approximately one hour at the workspace. The thickness of the Cu coating was measured every 50 cm along the foil length, starting at the 60 cm mark as shown in Figure 23a. Every 50 cm seven measurements have been taken across the foil width with 10 cm between measurement points. The foil areas with Cu thickness < 4 µm cannot be used for QH production and have to be removed. The Cu coating thickness profiles of the four quench heater foils are compared in Figure 24.
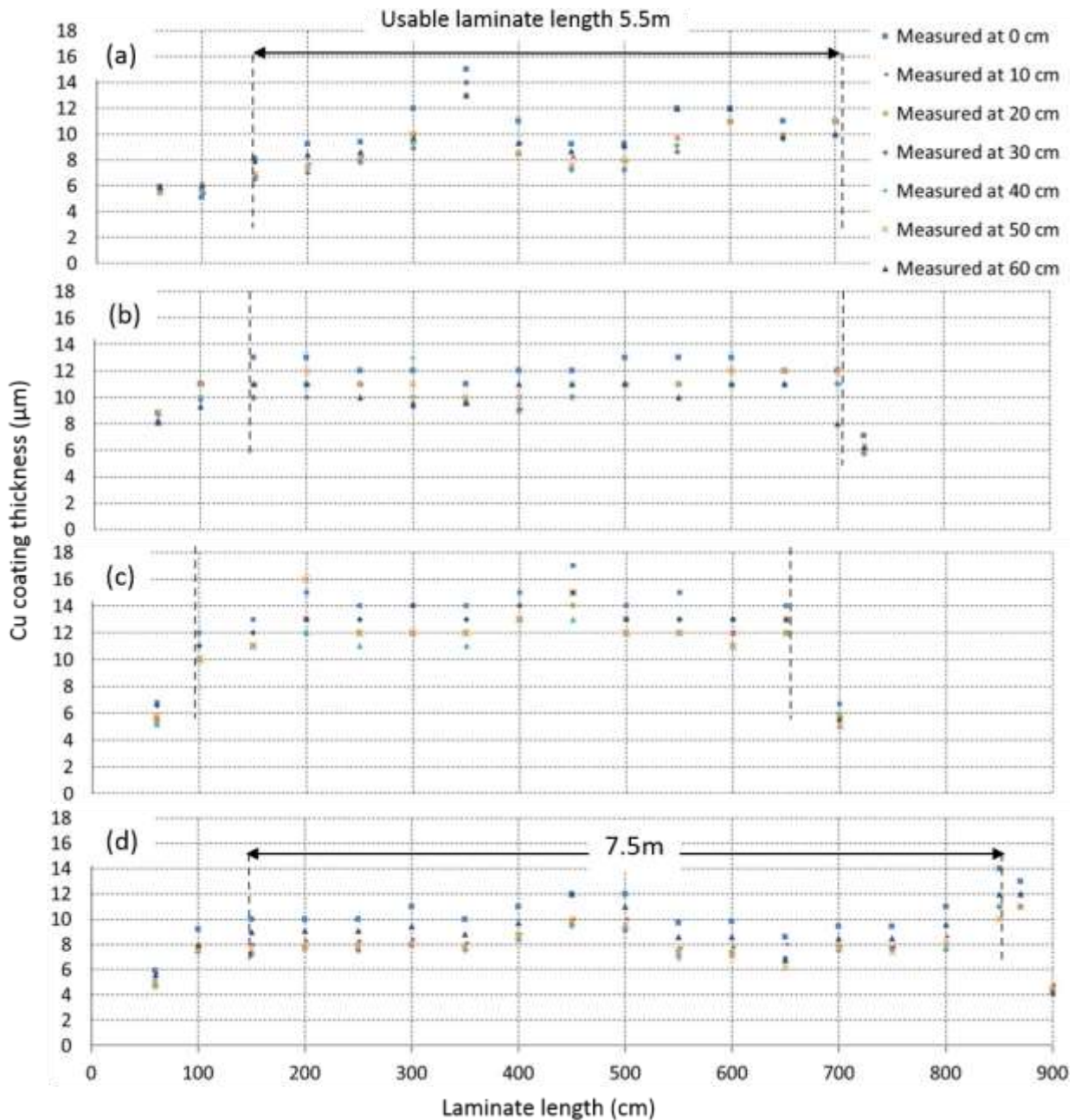
Figure 24: Cu coating thickness distribution on four different QH laminates, measured with Fischer SR-Scope. (a) 5.5m_001, (b) 5.5m_002, (c) 5.5m_003 and (d) 7.5m_001. The lines mark the required length for the production of two different QH types (11 T dipole and MQXF), and where the Cu coating thickness distribution has been calculated.

In Table 10 the Cu coating thickness distribution on the four laminates is compared. The standard deviation of the average thickness is a measure for the thickness variation on the different laminates. Within the usable length the Cu coating thickness varies between 6.1 to 17 µm. At least 50 cm on each end of the laminate are not well Cu coated and have to be cut, as well as approximately 1 cm

31

on each side of the substrate width cannot be used for QH production due to inconsistent Cu coating thickness or delamination.

Table 10: Summary of the Cu coating thicknesses measured with the Fischer SR-Scope on the four laminates. Thickness values are averaged over the usable length of the laminate and presented in μm ± 1 σ. Thickness values are not corrected for the influence of steel foil and Ni interlayer. The "average corrected" has been calculated according the Equation 1.

Foil ID	Maximum	Minimum	Average	Average corrected
5.5m_001	15	6.5	9.5±1.9	8.7
5.5m_002	13	8	10.9±0.6	10.1
5.5m_003	17	10	12.5±1.1	11.7
7.5m_001	14	6.1	8.9±1.3	8.1

A test report template has been developed (See Appendix 4) to report the results and any findings of the Cu coating characterisation. For the subsequent circuit etching process the Cu coating thickness distribution over the laminate is an important parameter. The thickness profile as shown in Figure 24 will be included in the report.

4.5.5 Cu coating thickness distribution on a finished quench heater circuit

The Cu coating thickness distribution has also been measured on the fully etched 4.8 m-long heater circuit that is shown in Figure 25. The steel-Polyimide laminate was Cu coated at the CERN PCB laboratory. During the subsequent photolithographic etching procedures, the relatively thick Cu oxide layer and an about 1 µm-thick Cu layer was removed.
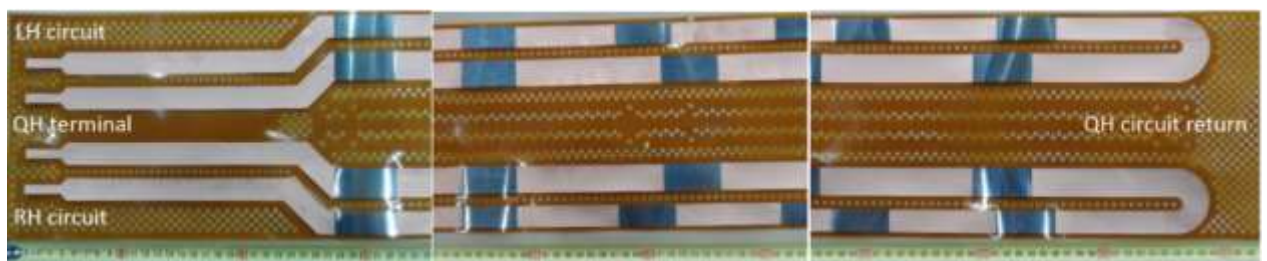
Figure 25: Quench heater circuit etched from the Cu coated Polyimide 304L steel laminate.

The 304L steel foil thickness of the heating stations was calculated from resistance measurements taken with the Megger DLRO 10 on the QH_Tr_001 LH circuit and the thickness profile is shown in Figure 26.
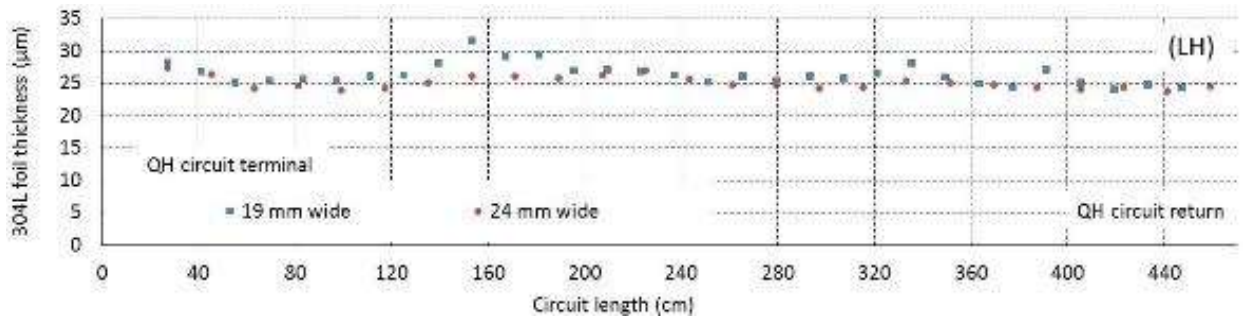
Figure 26: Thickness profile of the 304L steel foil segments on the QH_Tr_001 LH circuit.

The Cu coating thickness of the Cu coated segments was measured with the Fischer SR-Scope. Figure 27 shows the Cu coating thickness distribution on the LH and RH circuits of the QH_Tr_001.
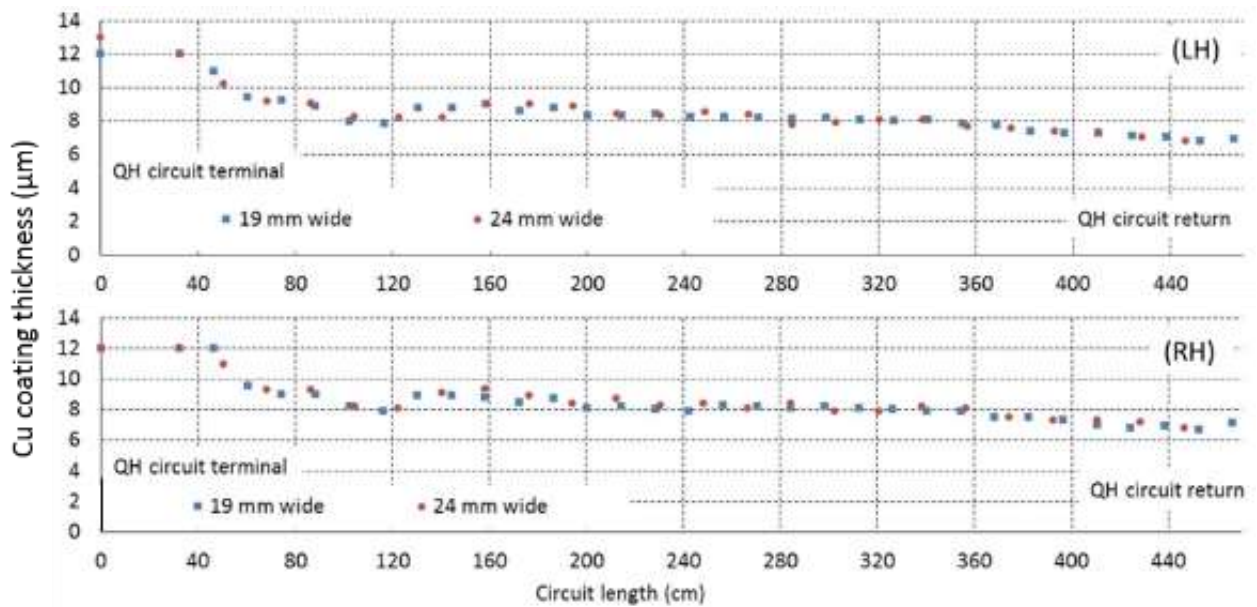
Figure 27: Cu coating thickness distribution on the LH and RH QH_Tr_001 circuit measured with the Fischer SR-Scope (without correction for the metal substrate influence). The measurements of the circuit return-end are included with the 19 mm wide segments.

For the average Cu coating thickness the measurement error due to the 304L foil and interlayer has not been considered. All measured results, the corrected average Cu thickness and maximum/minimum Cu thicknesses are listed in Table 11.

Table 11: Summary of the Cu coating thicknesses measured with the Fischer SR-Scope on the QH circuit as shown in Figure 25. Thickness values are averaged over the entire circuit in μm ± 1 σ. The "average corrected" has been calculated according the Equation 1.

	Maximum	**Minimum**	**Average**	**Average corrected**
QH_Tr_001 Left	13	6.8	8.5±1.3	7.7
QH_Tr_001 Right	12	6.7	8.5±1.3	7.7
QH_Tr_002 Left	13	6.6	8.5±1.3	7.6
QH_Tr_002 Right	13	6.7	9.0±1.4	8.2

4.6 Determination of the Cu coating adhesion

There are a number of standard tests to evaluate the adhesion of coatings to their substrate [25], [26], [27] (See also Appendix 5). Cu coating adhesion tests will be performed with the finished heater as it will be installed on the magnet coils. Destructive coating adhesion tests can be performed in different areas on the edges of the base material that are cut off before installation.

Two adhesion tests have been applied to various Cu coatings produced by electrolytic Cu deposition, E-beam evaporation and sputtering.

4.6.1 ASTM D6677 Standard Test for Evaluating Adhesion by Knife

The test sample is prepared with an "X"-shaped cut in the coating, using a scalpel and metal straight-edge. Legs of the "X" are about 40 mm long and crossing in an angle of 30° - 45°. The sharp edge of the knife is then used to peel off the coating, starting at the vertex of the angle.

A rating system is given, ranging in steps of 2 from 0-10. The coating is rated "0" if the coating can be easily detached and flakes greater than 6.3 mm in length can be peeled off. A rating of "10" is given for a coating that is very difficult to peel from the substrate, and if flakes occur they are smaller than 0.8 by 0.8 mm.
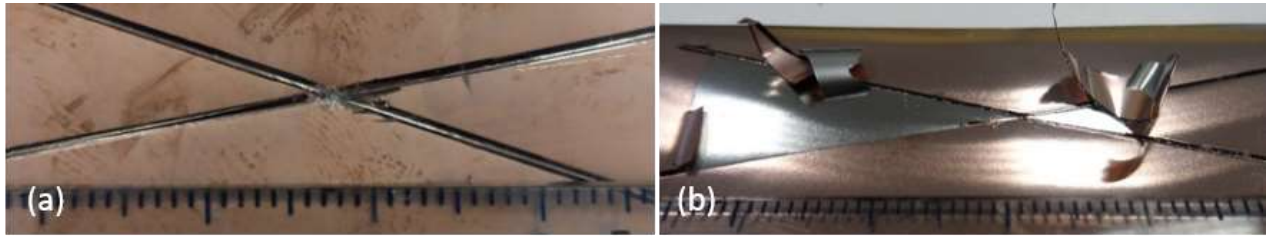
Figure 28: Example of different coatings tested according to ASTM D6677. (a) Electrodeposited Cu with no delamination of the Cu layer. (b) Sputter deposited Cu coating with low adhesion.

For the quench heaters only Cu coatings rated 10 according to ASTM D6677 are acceptable. Electrodeposited Cu coatings showed very high adherence to the 304L stainless steel surface (Figure 28a). The adherence of sputter deposited Cu coatings was very dependent on the coating process parameters, interlayers and substrate pre-treatment. Figure 28b shows a sputter deposited Cu coating with very low adhesion. Large flakes of coating could be easily peeled from the steel foil by hand. The silver underside of the flakes indicates low adhesion between the interlayer and the 304L foil. Other sputtered Cu coatings had adhesion comparable to the electrodeposited Cu. The E-beam evaporated Cu coatings showed varying adhesion just like the sputtered coatings, also very dependent on substrate pre-treatment and process parameters.

In Table 12 the different coatings are listed by manufacturing process with the results of the ASTM D6677 adhesion test.

Table 12: Results of the adhesion tests on Cu coatings from different manufacturers and Cu deposition technology.

Coating method	Supplier	Adhesion
Electrolytic	CERN PCB lab; 10 µm Cu+Wood's Ni+25 µm 304L+Polyimide	Excellent 10/10
	Lab1; 5 µm Cu+2 µm Ni+25 µm 304L+Polyimide	Excellent 10/10
Sputtering Cu onto diffusion barrier interlayer	CERN TE-VSC; 5 µm Cu + 0.5 µm Mo+25 µm 304L (before HT)	Excellent 10/10
	CERN TE-VSC; 5 µm Cu + 0.5 µm Mo+25 µm 304L after 650 °C HT	Excellent 10/10
	CERN TE-VSC; 5 µm Cu + 0.5 µm Ta+25 µm 304L (before HT)	Excellent 10/10
	CERN TE-VSC; 5 µm Cu + 0.5 µm Ta+25 µm 304L after 650 °C HT	Excellent 10/10
Sputtering	Lab2; 5 µm Cu + Ni+25 µm 304L+ Polyimide	Good 8/10
	Lab3; Cu+25 µm 304L+Polyimide	Poor 4/10
	Lab3; Cu+Cr interlayer+25 µm 304L	Poor 0/10
	Lab3; Cu+INCONEL600 interlayer+25 µm 304L+Polyimide	Poor 2/10
E-beam evaporation	Lab4; 1 µm Cu (2016-07-26A)	Excellent 10/10
	Lab4; 7.5 µm Cu (2016-08-10A)	Excellent 10/10
	Lab4; 7.5 µm Cu (2016-08-16A)	Poor 0/10

4.6.2 ASTM D4541 Pull-off strength of Coatings Using Portable Adhesion Testers (Test method F, self-aligning adhesion tester type VI)

The tests were conducted at the CERN VSC laboratory using a portable adhesion tester "PAThandy" from DFD instruments as specified in ASTM D4541-09, Test Method F, chapter A5 [26]. For this test a metal stud (Ø 5.7 mm) is glued to the test piece with epoxy glue (E1100S). The glue is cured in a furnace at 120°C -150°C-1 h in ambient atmosphere. Excessive glue is removed with a milling tool after curing. A washer is placed over the stud and the testing head is mounted. With the hydraulic pump pressure is applied on the four pins in the testing head, which lift the testing head with the stud off the coating.

Hydraulic pressure is increased until the stud detaches from the substrate or a designated pressure is reached. Figure 29 shows the PAThandy tester that was used for the test.

Figure 29: PAT handy adhesion tester in accordance with ASTM D4541 with the testing head for Ø 5.7 mm studs.

Two test runs have been performed with different coatings. The first test was carried out without sample preparation. Due to the inconsistent results the test was repeated with pre-cleaned samples, however, results could not be improved. The limiting factor in this test is suspected to be the flexible substrate which causes to deform and induces shear stresses that cause the stud to detach at very low forces. The oxidation of the Cu is suspected to be without influence on the test, since the epoxy adhesive prevented oxidation.
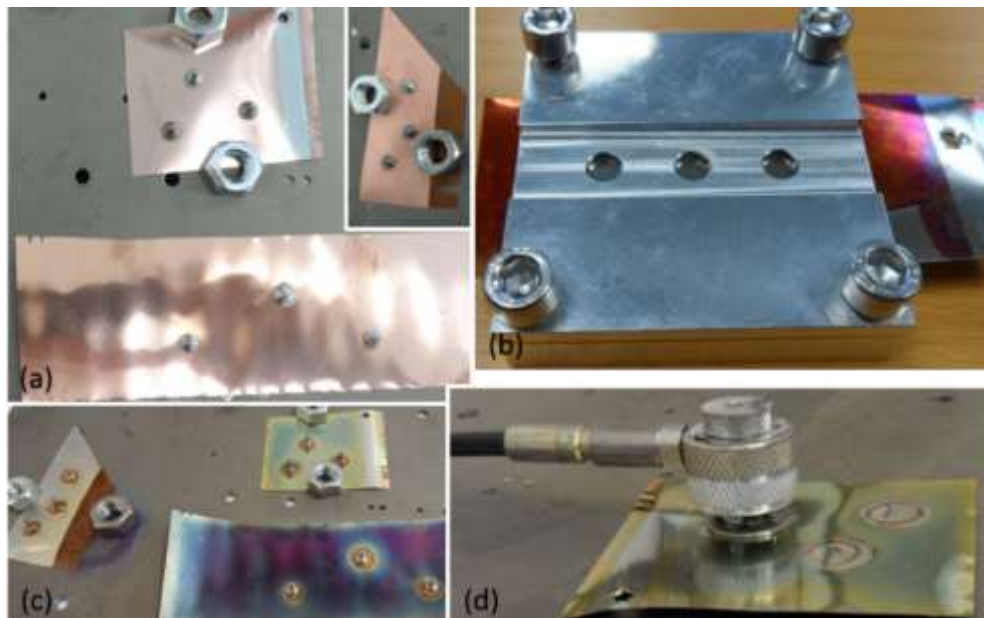
Figure 30: (a) Samples prepared with studs before heat treatment. (b) Fixture to support the sample during the adhesion test. (c) Samples after the HT. (d) Testing head mounted to the sample with a washer to support the push-pins.

A third test series was conducted using a sample fixture (Figure 30b, drawing in Appendix 3) to overcome the above suspected problem of sample flexibility. However, on all coatings tested the studs detached at low forces, and the Cu coating adhesion on the steel could not be tested.

From the test series it is concluded, that the standard test *"ASTM D4541 Pull-off strength of Coatings Using Portable Adhesion Testers"* is not suitable for testing the Cu coating adhesion on flexible QH substrates.

4.7 RRR measurements

The coating resistance of the QH is determined by the Cu coating geometry and the electrical resistivity of the Cu layer. At cryogenic temperatures where the QHs are operated, the electrical resistivity of pure Cu can be orders of magnitude lower than the RT electrical resistivity. The low temperature Cu resistivity is determined by RRR measurements, the RRR being defined as the ratio of the RT and 4.2 K resistance.

The RRR measurements are performed in the CERN Cryolab with three samples of each coating. The resistance of the samples is measured at 295 K in ambient air and at 4.2 K in liquid Helium with a test current of 100 mA. The sample holder is designed to carry three samples on each side (top and bottom in Figure 31b) and has integrated current leads, voltage taps and a thermometer to monitor the samples condition during the test. 100 mm long and 2 mm wide samples are cut and glued to a G10 strip before being mounted to the sample holder. Figure 31 shows the sample holder with voltage taps, current leads (a, b) and the samples glued to G10 (c). A Cu cylinder is mounted over the G10 sample holder before it is immersed into a cryostat with liquid helium.
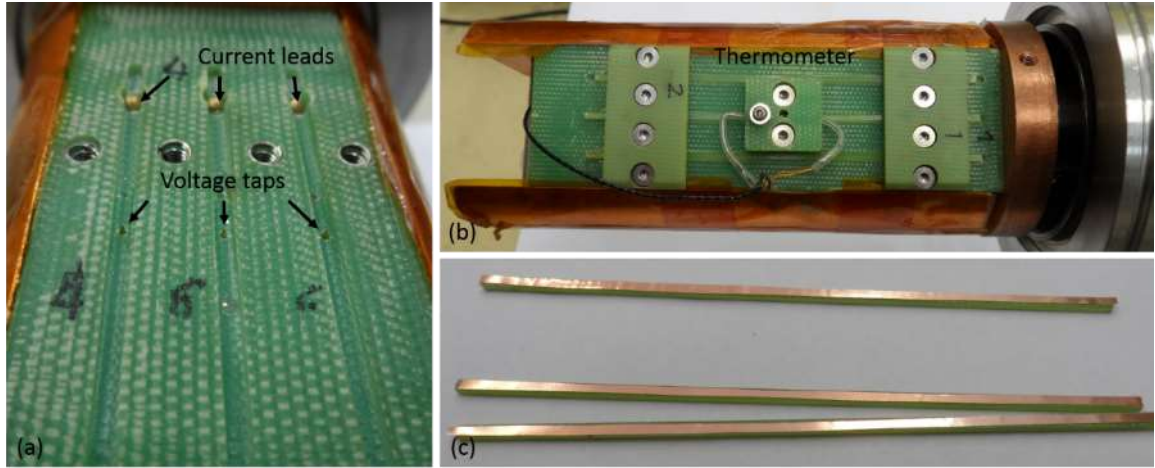
Figure 31: Sample holder for RRR measurements in the CERN Cryolab. (a)Current leads and voltage taps for the measurements. (b) Samples mounted to the holder with the thermometer. (c) Cu coating samples glued to G10 for reinforcement.

The RT electrical resistivity of the stainless steel substrate (0.73 Ωmm^2/m) is about 40 times higher than the Cu RT electrical resistivity (0.017 Ωmm^2/m). The relatively small influence on the RRR due to current flow through the steel substrate and interlayers is neglected. The RRR results of Cu coatings produced by different methods and manufacturers are summarised in Table 13. It can be seen that the Cu coating RRR depends strongly on the deposition process and process parameters.

Table 13: Summary of Cu coating RRR results.

Coating method	Sample	RRR
Electrolytic Cu	CERN PCB lab; 10 µm Cu+Wood's Ni+25 µm 304L+Polyimide	17.0±0.1
	Lab 1; 5 µm Cu+2 µm Ni+25 µm 304L+Polyimide	31±0.3
Sputtering	Lab 2; 5 µm Cu + Ni+25 µm 304L+Polyimide	2.3±0.05
	Lab 3; Cu+25 µm 304L+Polyimide	1.5±0.0
	Lab 3; Cu+Cr interlayer+25 µm 304L	2.3±0.02
	Lan 3; Cu+INCONEL600 interlayer+25 µm 304L+Polyimide	3.1±0.05
E-beam evaporation	Lab4; 1 µm Cu (2016-07-26A)	8.2±0.1
	Lab4; 7.5 µm Cu (2016-08-10A)	14.8±1.5
	Lab4; 7.5 µm Cu (2016-08-16A)	13.8±0.2

5 Development of HL-LHC 11 T dipole interlayer quench heater Cu coating with diffusion barrier interlayer

For the 11 T dipole magnets, interlayer quench heaters placed between the two coil layers during the coil winding process are considered. As described above the interlayer heaters would be subsequently subjected to the coil reaction heat treatment (HT) with a peak temperature of 650 °C. The standard HL-LHC quench heater materials (insulating Polyimide film and Cu coating) are not compatible with this HT. The maximum service temperature of the Polyimide would be exceeded and the diffusion of steel elements like Ni into the Cu layer would degrade its Residual Resistivity Ratio (RRR) to unacceptably low values. Therefore, a study has been undertaken to develop a Cu coating with a diffusion barrier interlayer that can resist the 650 °C HT.

Two potential barrier materials, notably Tantalum and Molybdenum, have been tested. The diffusion barrier layer is deposited by sputtering, which is a comparatively slow and expensive process. The diffusion barrier thickness can therefore have a strong influence on the cost of an industrial coating process. In order to determine the minimum diffusion barrier thickness, at the CERN VSC thin film laboratory 5 µm thick Cu coatings have been produced with interlayers of either Ta or Mo. The coatings have been characterised by means of RRR measurements, surface resistance measurements and by imaging of coating cross sections [28].

5.1 Cu coatings subjected to 650 °C HT

All coatings have been deposited onto a 25 µm-thick 304L steel foil. The Cu coatings with diffusion barrier have been produced by sputtering at the CERN VSC thin film laboratory. For comparison RRR measurements have been performed on two coatings without diffusion barrier, notably an electrolytic Cu coating produced at the CERN PCB laboratory, and an Electron-beam evaporated Cu coating.

The Cu coatings with Ta and Mo diffusion barrier have been deposited by magnetron sputtering onto chemically degreased steel foil 304L. A 135 °C-44 h bake-out of the coating system and substrate were performed prior to coating (limit pressure before coating in low 10^{-8} mbar range). During the deposition process the substrate temperature reached roughly 150–200 °C.

5.2   The heat treatment

The 650 °C-50 h HT has been performed at the CERN EN-MME soldering laboratory in a vacuum furnace. Figure 32 shows the coating samples placed inside the furnace (a) before and (b) after 650 °C-50 h HT. Visual inspection of the samples after HT shows that the sputter coated samples with diffusion barriers are deformed, while the other samples remained flat during the HT. The FEP and the CERN PCB samples show colour changes, presumably due to diffusion of steel substrate elements into the Cu coating.

① E-beam Cu on NiCr   ③ Sputtered Cu on 0.1 um Ta   ⑤ Sputtered Cu on 0.1 um Mo
② Electrolytic Cu; Wood's Ni   ④ Sputtered Cu on 0.2 um Ta   ⑥ Sputtered Cu on 0.2 um Mo
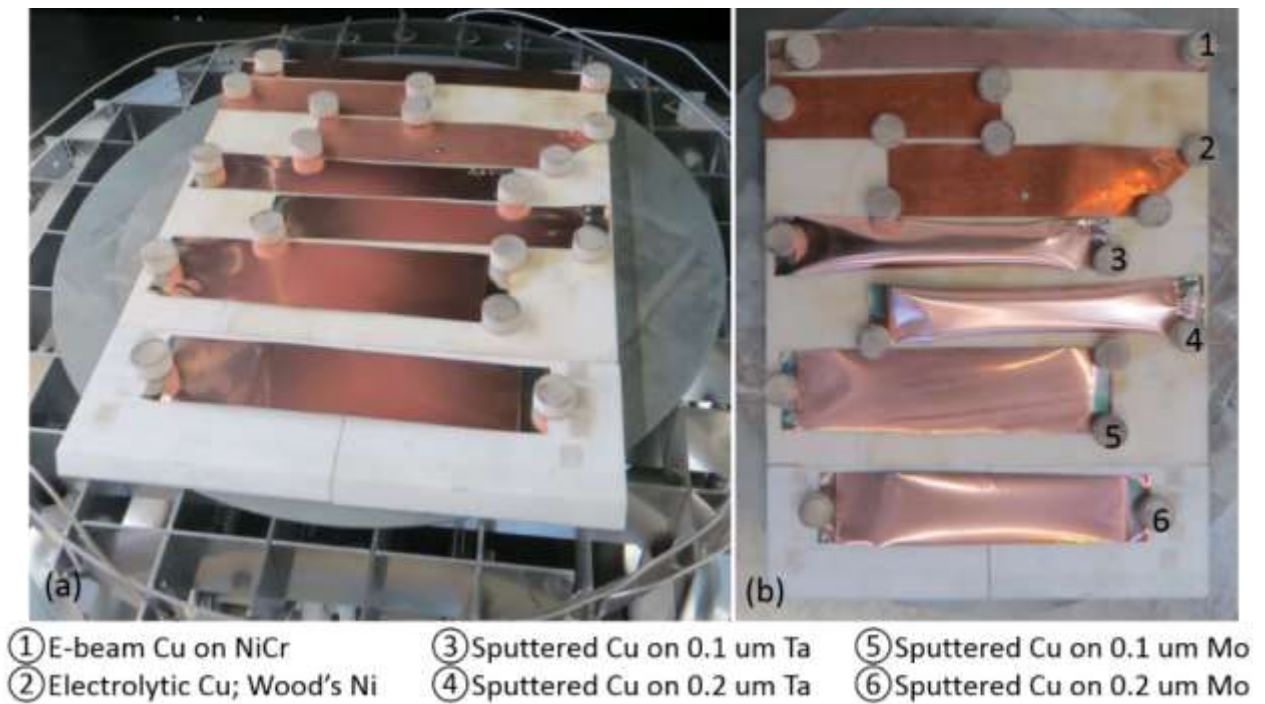
Figure 32: (a) Cu coated steel foils placed inside the vacuum furnace before the 650 °C-50 h HT. (b) Samples after 650 °C-50 h HT.

5.3   Influence of 650 °C-50 h HT on the Cu coating RRR

The RRR results of the different coatings before and after HT are summarised in Table 14 and in Figure 33. It can be seen that the Ta interlayers assure a high Cu RRR>30 after the HT. For all other samples the 650 °C HT causes a drastic RRR degradation.

Table 14: RRR of different Cu coatings before and after 650 °C-50 h HT in vacuum. All coatings are deposited onto a 25 μm thick 304L steel foil. *CERN PCB lab 10 μm electrodeposited Cu coating. **Sample 2016-08-10A, 7.5 μm E-beam evaporated Cu coating. *** CERN TE-VSC 5 μm sputter deposited Cu coating.

| Interlayer	RRR before HT	RRR after HT
Wood's Ni interlayer*	16±0.1	1.5±0.0
NiCr interlayer**	14±0.0	1.6±0.0
0.1 μm Ta diffusion barrier***	30±0.3	36±2.1
0.2 μm Ta diffusion barrier***	40±0.2	78±1.4
0.1 μm Mo interlayer***	41±1.1	1.6±0.0
0.2 μm Mo interlayer***	43±3.3	2.1±0.1
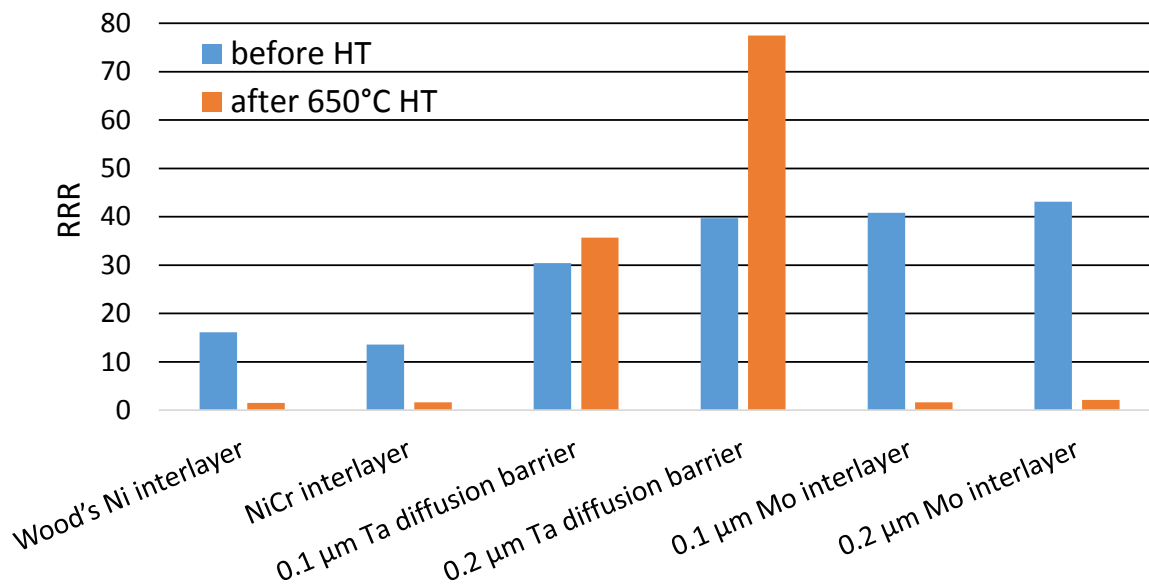
Figure 33: Influence of 650 °C-50 h HT on the RRR of Cu coated steel with different interlayers.

5.4 Cu coating surface resistance measurements

The Cu coating electrical resistance has been measured at RT before and after the 650 °C HT in order to determine the Cu coating thickness (Table 15). Measurements were taken with the Fischer SR-Scope and the Megger DLRO 10.

For the samples where a very low RRR indicates strong contamination of the Cu coating by interdiffusion with steel elements as a result of the 650 °C HT, no reliable thickness values could be derived. The RT resistivity of the coating was strongly increased with respect to the resistivity of pure Cu, making the thickness determination unreliable.

*Table 15: Cu coating thickness summary measured with Fischer SR-Scope. *CERN PCB lab 10 µm electrodeposited Cu coating. **Sample 2016-08-10A, 7.5 µm E-beam evaporated Cu coating. ***CERN TE-VSC 5 µm sputter deposited Cu coating.*

Interlayer	Cu thickness before HT (µm)	Cu thickness after HT (µm)
Wood's Ni interlayer*	9.6±0.2	n.m.
NiCr interlayer**	6.1±0.5	n.m.
0.1 µm Ta diffusion barrier***	6.1±0.6	5.2±0.5
0.2 µm Ta diffusion barrier***	6.3±0.8	6.7±0.6
0.1 µm Mo interlayer***	6.1±0.9	n.m.
0.2 µm Mo interlayer***	6.0±1.1	n.m.

5.5 Diffusion barrier integrity and coating morphology as observed by FIB-SEM

Figure 34 shows FIB-SEM cross sections of two sputter-coated Cu layers with 100 nm and 200 nm thick Mo interlayer after 650 °C-50 h HT. The Mo interlayers appear to have reacted with adjacent material, and are frequently interrupted. Furthermore, dark grains can be seen at the interface between the Cu surface and the protective platinum layer that is deposited prior to FIB cross section preparation. These grains are presumably formed from material that has diffused from the substrate through the Cu coating to the surface. The Cu coatings with Ni and NiCr interlayer exhibit a similar surface appearance after the 650 °C-50 h HT.
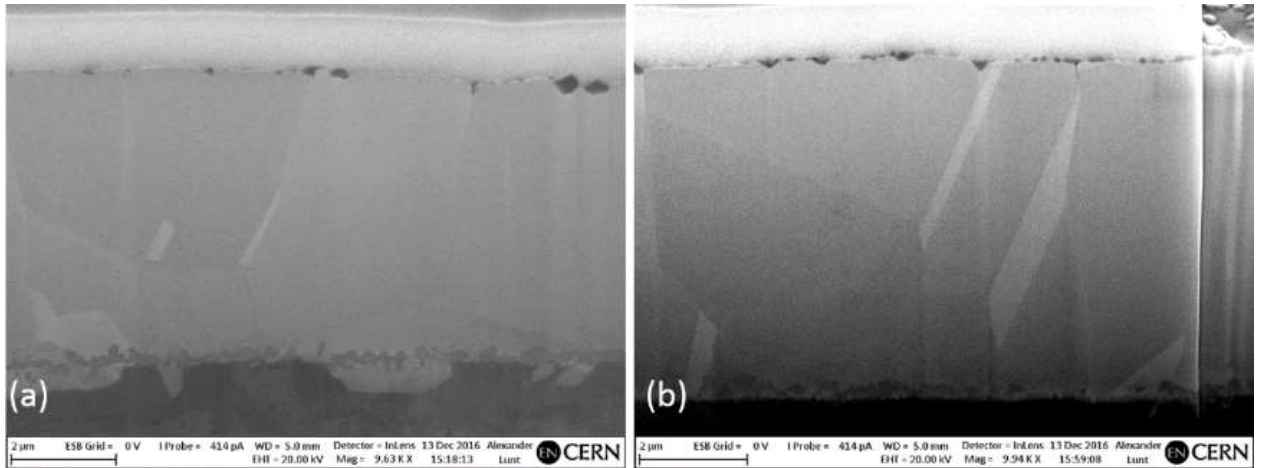
Figure 34: FIB-SEM cross section of sputter-coated Cu with (a) 100 nm-thick and (b) 200 nm-thick Mo interlayer after 650 °C-50 h HT.

A FIB-SEM cross section of a sputter-coated Cu layer with Ta interlayer after 650 °C-50 h HT is presented in Figure 35. In both cross sections the interlayer appears to be continuous, without large adjacent pores or impurities.
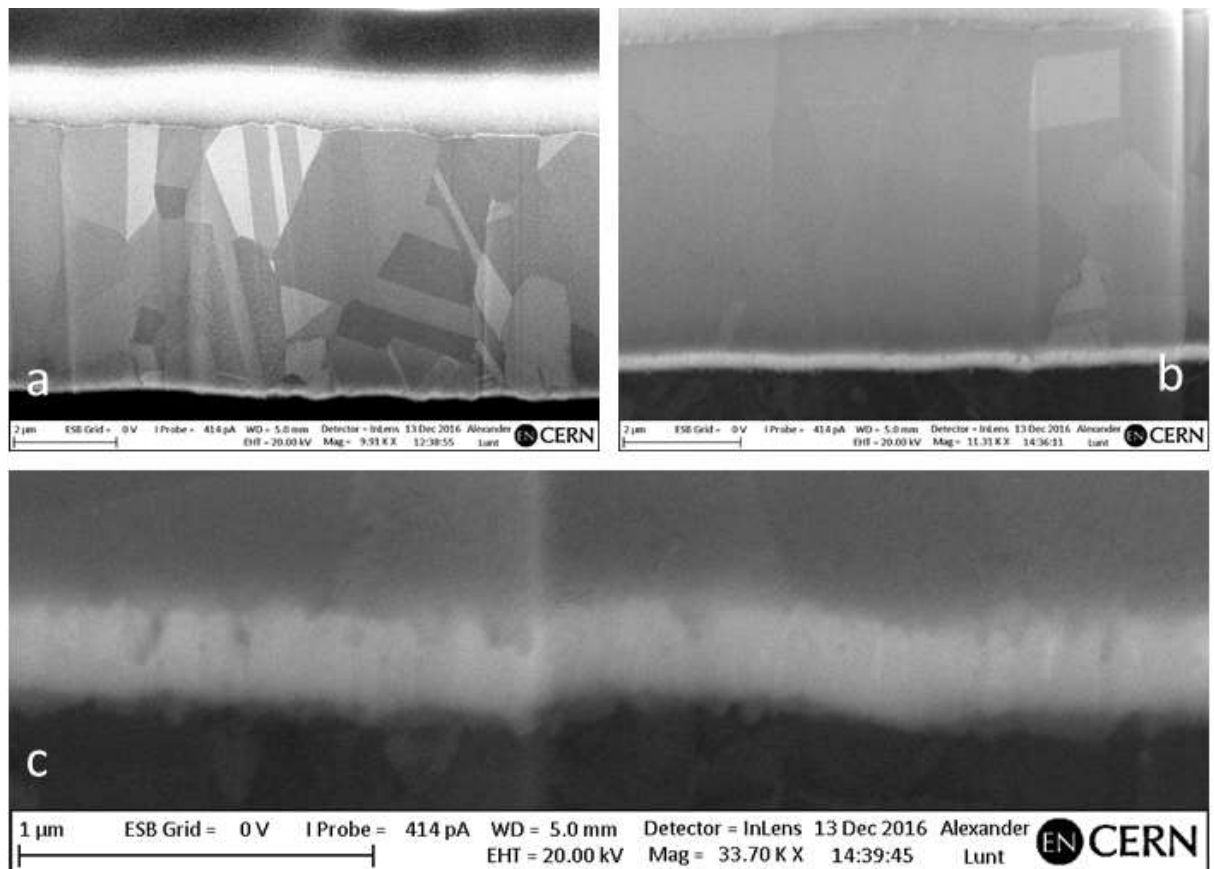

Figure 35: FIB-SEM cross section of a sputtered Cu coating with (a) 100 nm thick an (b,c) 200 nm-thick Ta diffusion barrier layer after 650 °C-50 h HT.

6 Discussion

Quench heaters are a crucial part of the protection system for the superconducting LHC magnets. This thesis focuses on the characterisation of QHs, and the evaluation of QHs produced using FPC production technology. Unlike the QH in the present NbTi LHC main dipole magnets, which are placed on the coil outer surface, the QH of the Nb_3Sn coils for the HL-LHC will be impregnated with the coil and repairs cannot be performed in case a defect is found. A high quality of the Polyimide 304L laminate and the Cu coating of the QHs is therefore a must.

The Cu coating of the steel-Polyimide laminate is the most critical part of the QH production. In particular the adhesion of the Cu coating to its substrate, and the Cu coating RRR are difficult to achieve on the large laminates needed for the QHs. The electrolytic Cu deposition multi pass roll-to-roll process as performed at the CERN PCB laboratory can provide up to 10 m-long, about 10 μm-thick Cu coatings with excellent adhesion and a sufficiently high RRR.

However, the production of the electrolytic Cu coating on the Polyimide 304L laminate poses further challenges, for instance to obtain a homogeneous Cu thickness distribution. The electrolyte bath used in the Cu coating process might possibly have an effect on the material properties of the Polyimide film and degrade the epoxy adhesive between Polyimide and 304L steel foil. This will be further investigated in future studies.

Cu coating by E-beam evaporation imposes a high heat load onto the Polyimide 304L laminate and can degrade the epoxy adhesive. As a solution it is considered to produce the E-beam evaporated Cu coating on a 304L foil that will be laminated to the Polyimide film in a subsequent production step.

The adhesion of most sputter coated Cu layers that have been studied here was insufficient. Only the coatings produced at the CERN thin film laboratory exhibited the required adhesion to the steel substrate. The RRR of the sputtered Cu coatings was very dependent on the process parameters, which have a direct effect on the Cu material structure. Cu coatings must have a dense material structure to achieve a RRR ≥10.

The RRR of the Cu coatings on steel with either Wood's Ni or NiCr interlayer degrades drastically during a 650 °C-50 h HT. Therefore, such coatings cannot be applied in interlayer quench heaters. Similarly the RRR of the Cu coating with a 100 nm and 200 nm thick Mo interlayer degrades from a RRR of about 40 before the HT, to a RRR of about 2 after the HT. FIB-SEM coating cross section analysis shows that the integrity of the Mo interlayer with 100 nm and 200 nm thickness is not

preserved during the 650 °C HT. Therefore, it is concluded that Mo is not a suitable diffusion barrier material between Cu and steel.

A Ta diffusion barrier layer of 100 nm thickness between the steel substrate and the Cu coating is efficient to keep a Cu coating RRR >30 after the 650 °C-50 h HT. The further coating development must assure the production of at least 6 m-long and 0.2 m-wide Cu coated steel foils from which the HL-LHC 11 T interlayer quench heater can be produced. In the further coating development, stresses in the steel-coating composite that may come for instance from the coating process, the thermal expansion mismatch of the composite materials or the steel substrate need to be considered as well.

The direct thickness measurements with micrometre and in FIB-SEM cross sections deliver comparable results to the indirect thickness determination by four-point electrical resistance measurements. The most efficient method is the thickness determination using the Fischer SR-Scope. The method allows to characterise a 7.5 m long QH laminate in approximately 20 minutes with about 100 measurement points. The measurement errors due to the electrically conductive interlayer and 304L foil are in the region of 8% for the required 10 µm-thick Cu coating. The developed correction factors to calculate the true Cu coating thickness of a Cu coating measured on a Polyimide 304L laminate with Ni interlayer and without interlayer are intuitive to apply.

The ASTM D6677 Adhesion test by knife allows to find coatings that have a very low adhesion. This destructive test can only be performed in areas that are not used for further QH production. The adhesion test using the PAThandy adhesion tester as specified in ASTM D4145 failed to deliver useful results presumably due to the flexible Cu coated Polyimide 304L laminate. It is, however, a useful test to determine a coating with very low adhesion, as shown on some of the sputter deposited Cu coatings.

The RRR measurements at the CERN cryolab are a crucial test to assure the good quality of the quench heater Cu coating. Samples need to be extracted from areas that do not interfere with the circuit routing.

7 Conclusion and outlook

Electrolytic Cu deposition can be conducted in a roll-to-roll process to produce the uniform Cu coating on several meter long QHs. The Cu coatings produced by electrolytic deposition fulfil the requirements for good adhesion if the 304L foil is pre-treated with a Wood's Ni strike. The Cu coatings have a dense material structure with material properties comparable to bulk Cu. The above

mentioned Cu coatings with Ni interlayer also meet the requirements of a RRR >10 for the quench heaters.

Cu coating by E-beam evaporation is considered as an alternative production technology. The substrate can also be Cu coated in a roll-to-roll process and the Cu material structure is comparable to that of electrolytic coatings. A RRR >10 and a good coating adhesion can be achieved.

Four-point electrical resistance measurements according to EN 14571:2005 using the Fischer SR-Scope measuring device have been found to be an efficient test to determine the Cu coating thickness distribution on the large flexible quench heater base material.

RRR measurements using 2 mm wide, 100 mm-long strips, which are cut from the QH base material, allow to determine the RT and 4.2 K electrical resistance of the Cu coating. Large variations of the Cu coating RRR have been observed, depending on the coating parameters.

The required good adhesion of the Cu coating to the steel substrate has been found to be most critical in the production process. Cu coating adhesion on the steel foil can be tested according to ASTM D6677 "Evaluating Adhesion by Knife". This destructive test can only be performed on laminate areas that are not used later on for the heater circuits. Most of the vacuum deposited coatings have not passed this adhesion test.

For the future QH routine quality controls, the tests for adhesion, as well as dielectric tests will be further refined. In order to compare the mechanical robustness of different heaters it is foreseen to perform tensile tests on the QH laminate and its constituents, at ambient temperature and in liquid nitrogen. Adhesion tests of the Cu coating and Polyimide 304L laminate will also be performed after thermal cycling by immersion of the QH in liquid nitrogen.

From the interlayer QH development study it is concluded, that a 0.1 µm-thick Ta diffusion barrier coating is sufficient to prevent strong Ni diffusion into the Cu layer and RRR degradation during a 650 °C-50 h HT.

The development of interlayer QHs will continue and should improve the magnet protection and provide redundancy. Interlayer QH technology relies on the further development of the Cu coating deposition by sputtering and E-beam evaporation. An electrical insulation scheme that can withstand the 650 °C-50 h HT needs to be developed and tested.

Appendix 1: Polyimide foil material datasheet

APICAL® AV

Kaneka

APICAL polyimide film possesses an excellent balance of physical, thermal, electrical and chemical properties over a wide range of temperature (-269°C [-452°F] to 400°C [752°F]). More precise thickness control, superior web flatness, plus improved adhesion and excellent dimensional stability are standard features with Apical polyimide films.

Major Applications
- Polyimide base materials for FPC.
- Motor generator insulation.
- Wire and cable insulation.
- Barcode label.
- Pressure sensitive tape.

Thermal Properties

Items	Units	Typical Values	Conditions	Methods
Coefficient of Thermal Expansion	ppm/°C	32	100 to 200°C	TMA

Chemical Properties

Items	Units	Typical Values	Conditions	Methods
Water Absorption	%	2.9	D-24/20	ASTM D-570
Coefficient of Humidity Expansion	ppm/%RH	16	50°C	HMA

Mechanical Properties

Items	Units	Typical Values	Conditions	Methods
Tensile Strength MD & TD	MPa	245	20°C	ASTM D882
Tensile Modulus MD & TD	GPa	3.1	20°C	ASTM D882
Elongation MD & TD	%	115	20°C	ASTM D882

Electrical Properties

Items	Units	Typical Values	Conditions	Methods
Volume Resistivity	Ωcm	$>10^{16}$	20°C	ASTM D-257
Dielectric Constant	-	3.3	20°C, 1 MHz	IPCTM-650
Dielectric Breakdown Voltage	V/μm	320	20°C, 60Hz	ASTM D-149

The data noted in these technical data sheets are given as examples and are not intended to be read as guaranteed values.

APICAL DIVISION - KANEKA TEXAS CORPORATION
6161 UNDERWOOD ROAD
PASADENA, TEXAS 77507
800-222-8128 FAX 800-562-5284
www.apicalpolyimide.com

Kaneka

Appendix 2: 11 T dipole quench heater drawing.

HILTI

11 T DIPOLE MEH

DER TE/HSE DUP

HEUNHEISD-THILL

50.0

90.0
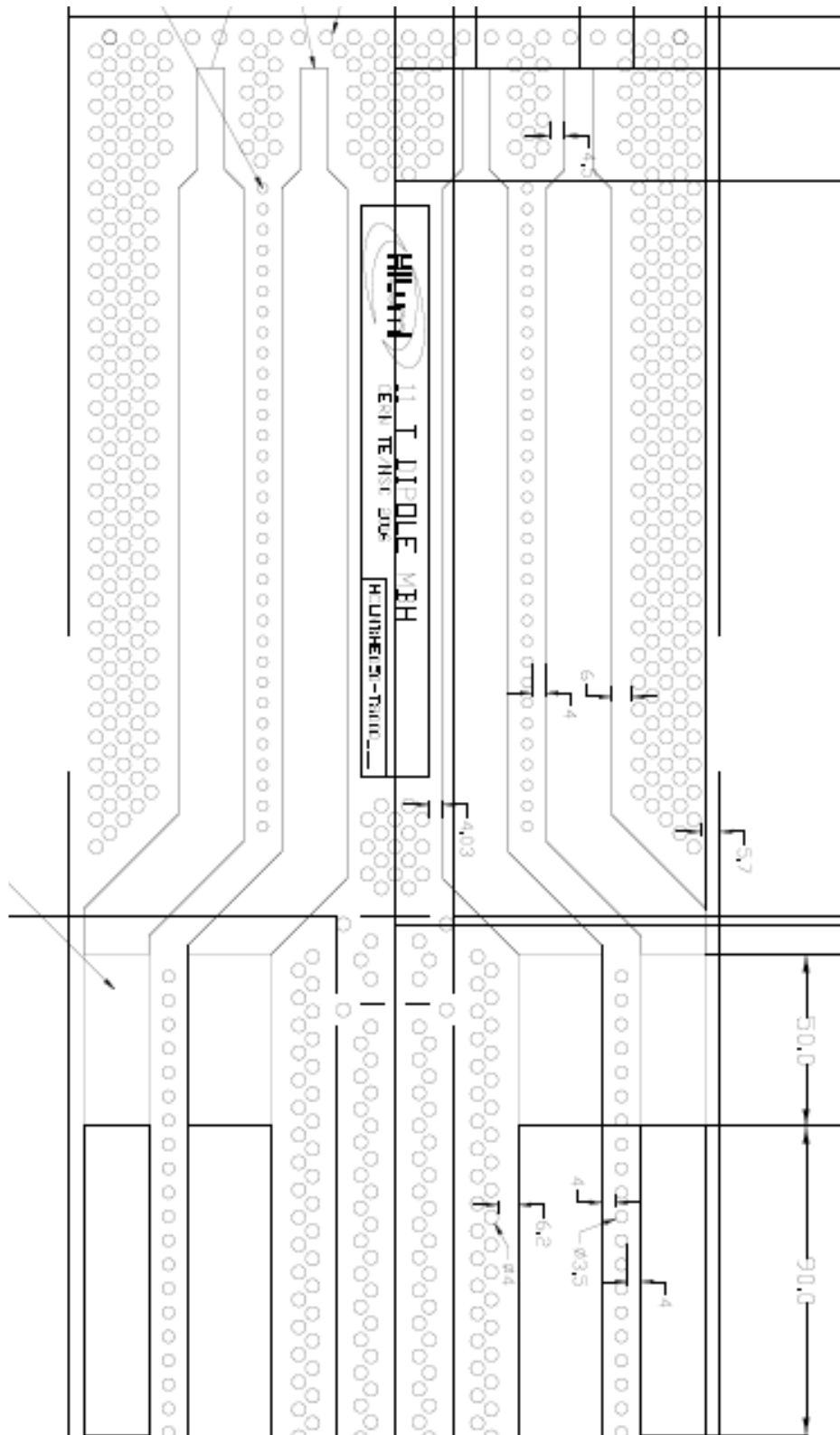
Appendix 3: Production drawing of the sample holder for adhesion tests
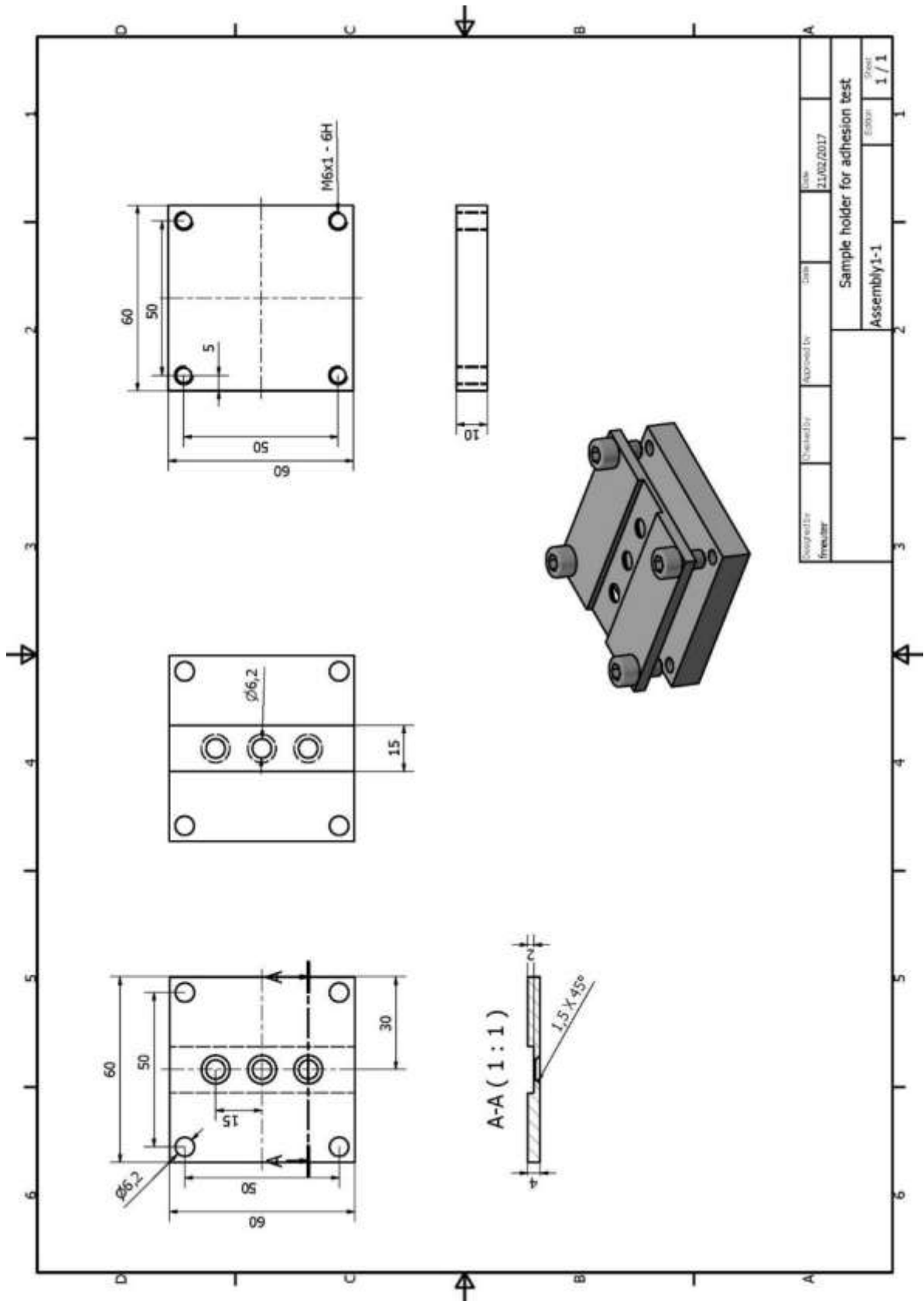
Appendix 4: Template for the Cu coating quality control tests

HL-LHC
11 T

Part ID		Drawing	
Template		Specification	

Quench heater laminate Cu coating characterisation

Ref. QH laminate:		Reception date:	
Cu coating manufacturer:		Operator:	

Quench heater laminate inspection:

Date of Test:		Equipment:	
Remarks:		Pictures:	

Overall length (cm):	Usable length (cm):

Cu coating thickness and RRR:

Ambient temperature (°C):		Equipment:	Fischer SR-Scope ERCU N
		Settings:	

Cu coating thickness (µm)			Calibration performed? Yes / No		

Minimum	Maximum	Average	Avrg. corrected	Correction factor for Cu thickness:	
				Ni interlayer	t_{Avr}-0.841
Cu coating RRR:				**NO interlayer**	t_{Avr}-0.567

Cu coating thickness profile:

Cu coating thickness (µm)

Laminate length (cm)

Appendix 5: ASTM standard adhesion test methods

ASTM D4541 Pull-off strength of Coatings Using Portable Adhesion Testers (Test method F, self-aligning adhesion tester type VI)

This adhesion test was developed to determine the pull-off strength of a coating on metal substrate. The test can be applied to determine the maximum perpendicular adhesive force between coating and substrate, or a coating can be assessed whether the coating adhesion will withstand a prescribed force specified by the application. This test is focused on the tensile stresses compared to the shear stresses applied in other methods such as Peel-off test or ASTM D6677 "Testing adhesion by knife". Therefore results of different tests need to be examined carefully as they may not be comparable.

The adhesion tester specified in ASTM D4541 applies a concentric load and counter load, so coatings can be tested from one side only. All test methods listed in ASTM D4541 require a dolly (or stud) to be glued normal to the coated surface. After curing the adhesive, the adhesion tester is mounted to the stud. The force is applied with a hydraulic pump, gradually increased and monitored until either the coating/the glue fails or a specified value is reached.

The tests were conducted at the CERN VSC laboratory using a portable adhesion tester "PAThandy" from DFD instruments as specified in ASTM D4541-09, Test Method F, chapter A5.

ASTM D3359 Measuring Adhesion by Tape Test

A very basic yet effective test is standardised in ASTM D3359. The test delivers quick but subjective results at minimum requirements by attaching adhesive tape to the coating and peeling it off.

The coating is prepared by making two 40 mm long cuts crossing in an angle of 30 °- 45°. Alternatively, if the test is performed in the laboratory an 11×11 square lattice can be cut with a 1 mm spacing between the lines (1 mm for ≤ 50 µm coating; 6×6 with 2 mm spacing for coating >50 µm).

After cleaning the surface from any chips and shavings, adhesive, pressure sensitive tape of 75 mm length and 25 mm width is placed over the cuts and properly adhered by using a rubber eraser. The specification of the tape is discussed beforehand (e.g. Permacell 99 or equivalent). The tape is then peeled off backwards in a steady and fast motion.

The area is then examined for flaking and separation of the coating. A classification scale can be found in ASTM D 3359 ranging from 0A (large area peeled off) to 5A (no peeling) for test Method A (X – cut).

For test method B (lattice cut) a range from 0B (65% of the cross cut area has separated) to 5B (no separation) is specified.

ASTM D2197-98 Test Method for Adhesion of Organic Coatings by Scrape Adhesion

Although specified for organic coatings this test might be a suitable method to evaluate the adhesion of the Cu coating on the 304L foil.

This test requires a setup (scrape adhesion tester) consisting of a beam holding a scraping loop. The beam has a platform to accommodate weights that exert a force on the scraping loop. The scraping loop is then lowered onto the sample and moved over it at least 75 mm with the force applied.

The load is increased or decreased until the coating is damaged or the maximum load of 10 kg is reached.

This test certainly requires a solid backing and solid fixture of the sample before tests can be performed.

ASTM B571 – 97 Standard Practice for Qualitative Adhesion Testing of Metallic Coatings, Bend Test

The laminate is bend over a mandrel with a diameter 4× the laminate thickness. During bending the coated surface is facing away from the mandrel and the sample will be bend 180º until both legs are parallel. The coating is then examined (low magnification if necessary) for delamination, flaking and cracks. The tip of a knife can be used to peel flakes if necessary.

Appendix 6: Coating thickness test methods

EN ISO 1463 Metallic and oxide coatings - Measurement of coating thickness - Microscopical method

The standard specifies the procedure to measure the coating thickness by optical microscope. This inspection requires extensive preparation of the sample prior to inspection. Especially in case of the thin polyimide-304L-Cu laminate a solid backing would be required or alternatively embedding the sample in a support material. The embedded sample will then be polished to remove deformations in the cut edge. To improve contrast between laminations the cut edge will be etched. The sample can then be inspected under a microscope. Due to the extensive sample preparation and limited sample size it is a good test for initial coating inspection but is not a suitable test for continuous quality control.

ISO 4518 Metallic coatings - Measurement of coating thickness - Profilometric method

This procedure allows measurements from 0.01 µm – 1000 µm [29] coating thickness with acceptable results. The test requires a defined step in the coating by either removing parts of it or by covering the area to be inspected before coating is applied. Afterwards the height of this step is measured by tracking the deflection of the probe.

ISO 2177 Metallic coatings – measurement of coating thickness – Coulometric method by anodic dissolution

This method requires electrolytic removal of a defined sample size. By measuring the current and time necessary to dissolve the coating the thickness can be determined. When the coating is completely dissolved the potential will change and will be recognized by the test equipment. The error of this procedure is less than 10 % of the coating thickness [30,31].

Alternatively the sample can be weighed before and after removal of the coating and with knowledge of the coatings density the thickness can be calculated.

Instead of weighing the sample, it can be completely dissolved and the solution will then be chemically analysed for traces of the materials (ISO 10111).

ISO 2360:2003 Non-conductive coatings on non-magnetic electrically conductive basis material – Measurement of coating thickness – Amplitude sensitive eddy-current method

The eddy current method is capable of measuring coating thickness of ≥ 5 µm with acceptable accuracy if the average of several measurements is taken. Above 25 µm coating thickness the method related error depends on the thickness. However this method is dedicated for inspection of non-conducting coatings on non-magnetic substrate. Measurements for metallic coating on metallic substrate are possible but results are difficult to achieve [32].

ISO 3497 Metallic coatings - Measurement of coating thickness - X-ray spectrometric methods

For an x-ray fluorescence analysis the material is first locally exposed to gamma- or x-rays, called primary radiation, that ionize the atoms and expel electrons. The atom becomes unstable and in order to gain back stability, electrons from higher shells replace the expelled electrons. The "falling" electrons release energy in form of photons. The energy of the radiation of photons is measured by a detector and is characteristic for each element. From the amount of emitted radiation the coating thickness can be calculated as well as the coating materials composition. Before the actual sample can be inspected the machine needs to be calibrated with a reference sample that is well known in its composition and dimensions. This method can be considered an applicable method for thickness determination on the Cu coated laminate, however it requires extensive equipment and maximum sample size has to be determined. In return this method is capable of measuring even very thin coatings or just traces of elements in a coating.

References

1 LHC Design Report Vol.1, *"The LHC Main Ring"*, edited by O. Brüning, P. Collier, P.Lebrun, S. Myers, R. Ostojic, J. Poole, P. Proudlock, CERN-2004-003, (2004)

2 L. Rossi, "S*uperconductivity: its role, its success and its setbacks in the Large Hadron Collider of CERN"*, Superconductor Science and Technology, 23(3), 2010

3 *"The High luminosity Large Hadron Collider"*, Editors O. Brüning, L. Rossi, World Scientific Publishing Co.Pte.Ltd. Singapore, 2015

4 L. Bottura, G. de Rijk, L. Rossi, E. Todesco, *"Advanced accelerator magnets for upgrading the LHC"* IEEE Trans. Appl. Supercond., vol. 22, no. 3, June 2012, 4002008

5 F. Rodriguez-Mateos et al, *"Quench Heater Experiments on The LHC Main Dipole Superconducting Magnets"*, LHC Project Report 418

6 M. Karppinen et al., *"Design of 11 T twin-aperture dipole demonstrator magnet for LHC upgrades"*, IEEE Trans. App. Supercond., vol. 22, no. 3, June 2012

7 Quench heater discharge power supplies for the protection of LHC superconducting magnets. (http://te-epc-lpc.web.cern.ch/te-epc-lpc/converters/qhps/general.stm) 09.02.2017

8 *"Technical Specification for the Supply of Quench Heaters for the series LHC Superconducting Main Dipole Magnets"*, CERN EDMS No. 316296

9 B. Szeless et al., *"Development of Industrially Produced Composite Quench Heaters for the LHC Superconducting Lattice Magnets"*, LHC Project Report 48

10 S. Izquierdo Bermudez, CERN, private communication

11 S. Izquierdo Bermudez et al., *"Quench Protection Studies of the 11-T Nb3Sn Dipole for the LHC Upgrade"*, IEEE Trans. App. Supercond., Vol. 26, no. 4, June 2016

12 Andries den Ouden, Herman H.J. ten Kate *"Thermal Conductivity of Mica/glass Insulation for Impregnated Nb3Sn Windings in Accelerator Magnets"*

13 P.Macleod "*A Review of Flexible Circuit Technology and its Applications*", (www.lboro.ac.uk/Technology_review/flexible-circuit-technology-and-its-applications.pdf) 21st February 2017

14 Kaneka Apical AV data sheet (www.kanekatexas.com), 21st February 2017

15 Film materials for flexible printed circuit production (http://www.gts-flexible.com) 21st February 2017

16 "*Rolle-zu-Rolle Pilotbandbeschichtungsanlage novoFlex®600*", Fraunhofer-Institut für Organische Elektronik, Elektronenstrahl- und Plasmatechnik FEP (www.fep.fraunhofer.de/de/Leistungsangebot/Anlagentechnik.html), 8th February 2017

17 F. Meuter, C.Scheuerlein, "*Thickness measurement of the Cu coating on the Polyimide-steel laminate for the HL-LHC quench heaters",* Technical Note 2017_03 CERN EDMS No. 1759728

18 DIN 863-1 "*Verification of geometrical parameters –Micrometers-Part 1*": Standard design micrometers callipers for external measurements – Concepts, requirements, testing; April 1999

19 Standard EN 14571:2005 "*Metallic coatings on nonmetallic basis materials-Measurement of coating thickness-Microresistivity method*"

20 Handbook of Chemistry and Physics, 76th edition, edited by D.R. Lide and H.P.R. Frederikse, CRC Press, Inc., 1995

21 W. Hesse, *"Material data sheets Non-ferrous metals";* 1st edition 2014, Beuth Verlag GmbH

22 Material data sheet ACIDUR 4307 (1.4307); (www.dew-stahl.com) June 28th 2016

23 DLRO 10X Digital Micro-ohmeter (ww.megger.com) 21st February 2017

24 Fischer SR-Scope, Measurement of Cu thickness on PCBs – Micro-resistivity method (www.fischer-technology.com) 21st February 2017

25 ASTM D3359 "*Measuring Adhesion by Tape Test"*

26 ASTM D4541 "*Pull-off strength of Coatings Using Adhesion Tester"* (Test Method F, self-aligning adhesion tester type VI)

27 ASTM D6677 *"Standard Test Method for Evaluating Adhesion by Knife"*

28 F. Meuter, C.Scheuerlein, W.Vollenberg "*Development of HL-LHC 11 T dipole interlayer quench heater Cu coating with diffusion barrier interlayer",* Technical Note 2016_12 CERN EDMS No. 1744302

29 EN ISO 4518:1995 *"Metallic coatings – Measurement of coating thickness*" – Profilometric method

30 ISO 2177 *"Metallic coatings – Measurement of coating thickness"* – Coulometric method by anodic dissolution

31 C. Scheuerlein, G. Arnau, N. Charras, L. Oberli, M. Taborelli, "*The thickness measurement of Sn-Ag coatings on LHC superconducting strands by coulometry*", J. Electrochem. Soc., 151, (2004), 206

32 ISO 3882:2003 *"Metallic and other inorganic coatings"* – Review of methods of measurement of thickness